NASA TECHNICAL NOTE

NASA TN D-6118

C.1

NASA TN D-6118

A WIND-TUNNEL INVESTIGATION OF HELICOPTER DIRECTIONAL CONTROL IN REARWARD FLIGHT IN GROUND EFFECT

by Robert J. Huston and Charles E. K. Morris, Jr.

Langley Research Center
Hampton, Va. 23365

NATIONAL AERONAUTICS AND SPACE ADMINISTRATION • WASHINGTON, D. C. • MARCH 1971

1. Report No. NASA TN D-6118	2. Government Accession No.	3. Recipient's Catalog No.
4. Title and Subtitle A WIND-TUNNEL INVESTIGATION OF HELICOPTER DIRECTIONAL CONTROL IN REARWARD FLIGHT IN GROUND EFFECT		5. Report Date March 1971
		6. Performing Organization Code
7. Author(s) Robert J. Huston and Charles E. K. Morris, Jr.		8. Performing Organization Report No. L-7432
9. Performing Organization Name and Address NASA Langley Research Center Hampton, Va. 23365		10. Work Unit No. 721-60-10-01
		11. Contract or Grant No.
12. Sponsoring Agency Name and Address National Aeronautics and Space Administration Washington, D.C. 20546		13. Type of Report and Period Covered Technical Note
		14. Sponsoring Agency Code
15. Supplementary Notes		

16. Abstract

An investigation was conducted in the Langley full-scale tunnel to study the aerodynamics that produce directional-control problems for a helicopter with a tail rotor in low-speed rearward flight in ground effect. A helicopter model mounted close to the tunnel floor was tested in tail winds from 0 to 25 knots.

17. Key Words (Suggested by Author(s)) Directional control; Helicopter tail rotors; Ground effects; Fin interference	18. Distribution Statement Unclassified – Unlimited

19. Security Classif. (of this report)	20. Security Classif. (of this page)	21. No. of Pages	22. Price*
Unclassified	Unclassified	38	$3.00

*For sale by the National Technical Information Service, Springfield, Virginia 22151

A WIND-TUNNEL INVESTIGATION OF HELICOPTER DIRECTIONAL CONTROL IN REARWARD FLIGHT IN GROUND EFFECT

By Robert J. Huston and Charles E. K. Morris, Jr.
Langley Research Center

SUMMARY

An investigation was conducted in the Langley full-scale tunnel to study the aerodynamics that produce directional-control problems for a helicopter with a tail rotor in low-speed rearward flight in ground effect. A helicopter model mounted close to the tunnel floor was tested in tail winds from 0 to 25 knots.

Results identified significant adverse effects of the main-rotor wake that include an increase in the adverse fin force, a decrease in the tail-rotor thrust obtained, and an increase in tail-rotor torque required. The adverse effects are the result of the immersion of the tail rotor and fin in a ground vortex generated by the interactions of the main-rotor wake and the wind in the presence of the ground. When rearward airspeed is sufficiently increased, the free-stream flow diminishes the ground vortex and carries it away from the tail rotor and fin; as a result, there is an abrupt change in tail-rotor collective pitch required that simulates flight results.

INTRODUCTION

Directional-control problems in hovering or low-speed flight have commonly occurred with new helicopter designs. In one specific case, a single-rotor helicopter was found to have inadequate directional control when hovering in a low-velocity left-rear-quartering wind. (See ref. 1.) Usual approaches to solutions for such problems have been a series of apparently random changes in the tail-rotor configuration: a tail rotor originally designed to be on one side of the fin is moved to the opposite side; the direction of rotation is reversed; the vertical fin is lengthened or bobbed; or a new trailing edge is affixed. This random treatment of tail-rotor parameters reflects the limited knowledge of the tail-rotor operational environment. Prior to the publication of reference 2, which includes part of this paper, little published information was available to guide the design of tail-rotor configurations of helicopters to minimize low-speed directional-control problems.

The aerodynamic environment in which the tail rotor operates is extremely complicated, and few measurements exist of tail-rotor performance in the rearward-flight region. The tail rotor operates close to the main rotor; therefore, there could be a strong interaction between the two wakes. The tail rotor is usually mounted on the side of a vertical fin which blankets 15 to 25 percent of the tail-rotor area, and thereby requires an azimuthal concentration of the tail-rotor inflow to regions forward and aft of the fin. Variable winds and pilot-directed control of the helicopter heading can contribute to the uncertainty of flight measurements in a regime where the flow is unsteady and the aircraft is inherently unstable. Additional complications include the uncertainty of ground-induced turbulence, the mixing of rearward-directed engine-exhaust air, and the normal lack of adequate measurements of the vehicle's velocity at low speeds. Obviously, it is difficult for flight measurements to provide an understanding of the phenomena that produces directional-control problems with helicopters in hovering or low-speed rearward flight.

In order to provide some understanding of the tail-rotor operating conditions, it was considered necessary to obtain simultaneous and detailed measurements of forces and moments of the tail rotor, main rotor, and fin under closely controlled conditions. Accordingly, a helicopter model, mounted on the ground board of the Langley full-scale tunnel, was tested in tail winds ranging from 0 to 25 knots. The model was tested both with the main rotor stopped and with it operated at constant lift. Tail-rotor collective pitch was varied at each wind speed in order to bracket yaw-trimmed flight conditions.

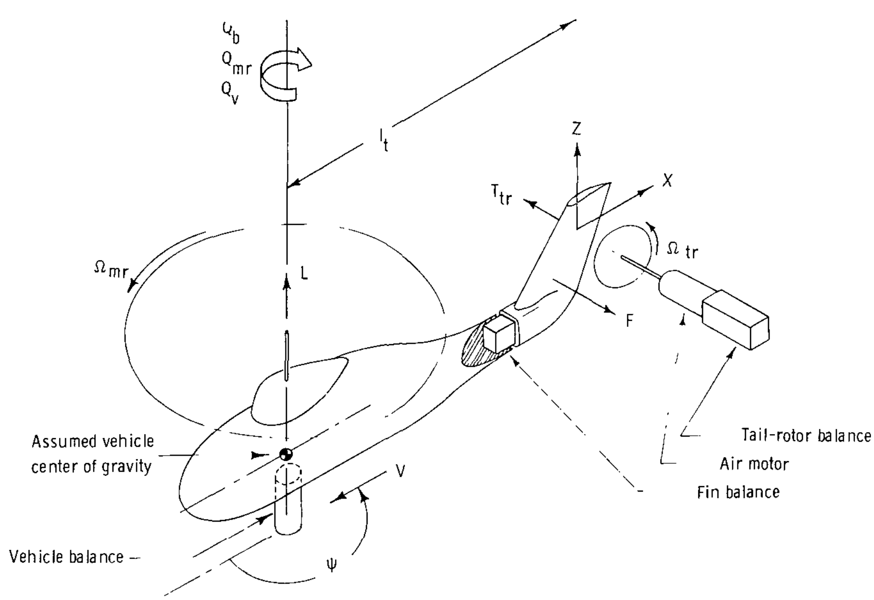

Figure 1.- Model schematic and conventions used to define positive sense of forces and moments.

SYMBOLS

The positive senses of forces, moments, and displacements are indicated in figure 1. The measurements and calculations were made in U.S. Customary Units. The physical quantities used in this paper are given in both the International System of Units (SI) and U.S. Customary Units. Factors relating the two systems are given in reference 3.

C_F fin-force coefficient, $\dfrac{F}{\pi R_{tr}^2 \rho (\Omega R)_{tr}^2}$

C_L' main-rotor lift coefficient, $\dfrac{L}{\pi R_{mr}^2 \rho (\Omega R)_{mr}^2}$

$C_{Q,b}$ fuselage torque coefficient, $\dfrac{Q_b}{\pi R_{mr}^3 \rho (\Omega R)_{mr}^2}$

$C_{Q,mr}$ main-rotor torque coefficient, $\dfrac{Q_{mr}}{\pi R_{mr}^3 \rho (\Omega R)_{mr}^2}$

$C_{Q,tr}$ tail-rotor torque coefficient, $\dfrac{Q_{tr}}{\pi R_{tr}^3 \rho (\Omega R)_{tr}^2}$

$C_{Q,v}$ vehicle torque coefficient, $\dfrac{Q_v}{\pi R_{mr}^3 \rho (\Omega R)_{mr}^2}$

$C_{T,tr}$ tail-rotor thrust coefficient, $\dfrac{T_{tr}}{\pi R_{tr}^2 \rho (\Omega R)_{tr}^2}$

C_σ torque-balance coefficient (value of 1 indicates vehicle is trimmed in yaw), $\dfrac{l_t T_{tr}}{Q_v}$

c rotor-blade chord, meters (feet)

F fin force, newtons (pounds force)

L main-rotor lift, newtons (pounds force)

l_t horizontal distance from tail-rotor shaft to main-rotor shaft and assumed vehicle center of gravity, meters (feet)

Q_b fuselage torque, newton-meters (foot-pounds force)

Q_{mr} main-rotor shaft torque, newton-meters (foot-pounds force)

Q_{tr} tail-rotor shaft torque, newton-meters (foot-pounds force)

Q_v vehicle torque (sum of fuselage, main rotor, and vertical fin torque), newton-meters (foot-pounds force)

R rotor radius, meters (feet)

T rotor thrust, newtons (pounds force)

V free-stream velocity, knots

X,Z coordinate axes on vertical fin orthogonal to tail rotor thrust axis

x_a coordinate of airfoil section, measured from leading edge rearward, meters (feet)

x_{cp} longitudinal coordinate for center of pressure on vertical fin, measured from center of tail rotor, meters (feet)

y_a thickness coordinate of airfoil section, measured perpendicular from chord line, meters (feet)

z_{cp} vertical coordinate for center of pressure on vertical fin, measured from center of tail rotor, meters (feet)

θ rotor-blade collective pitch angle, degrees

ρ mass density of air, kilograms per meter^3 (slugs per foot^3)

ψ angle of yaw, degrees

Ω rotor rotational speed, radians per second

Subscripts:

mr main rotor

tr tail rotor

MODEL DESCRIPTION AND TEST PROCEDURE

Model

A drawing of the model used in this investigation is presented in figure 2, and photographs of the model are shown in figure 3. The fuselage assembly, which included the main rotor and vertical fin, was mounted on a six-component strain-gage balance attached to the top of a pedestal. The pair of variable-speed electric motors that drove the main rotor were mounted within the fuselage body. The tail rotor and the air motor that powered that rotor were mounted on a six-component strain-gage balance attached to the end of a horizontal sting. The horizontal sting was attached to the top of a pedestal which was 1.14 meters (3.75 feet) from the vertical fin.

The main rotor and tail rotor were two-bladed, teetering rotors. Both rotors were equipped with remote collective-pitch controls. In addition, the main rotor was provided with longitudinal- and lateral-cyclic pitch control through a remotely operated, conventional swashplate system. Other characteristics of the rotors are listed in table I. The airfoil section coordinates of the main rotor are given in table II.

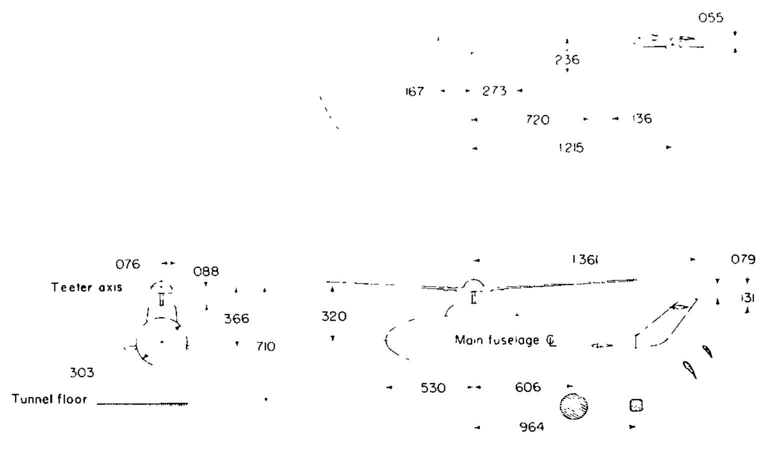

Figure 2.- Three-view drawing of model. All dimensions given are ratios of main-rotor radius. R_{mr} = 1.68 m (5.50 ft).

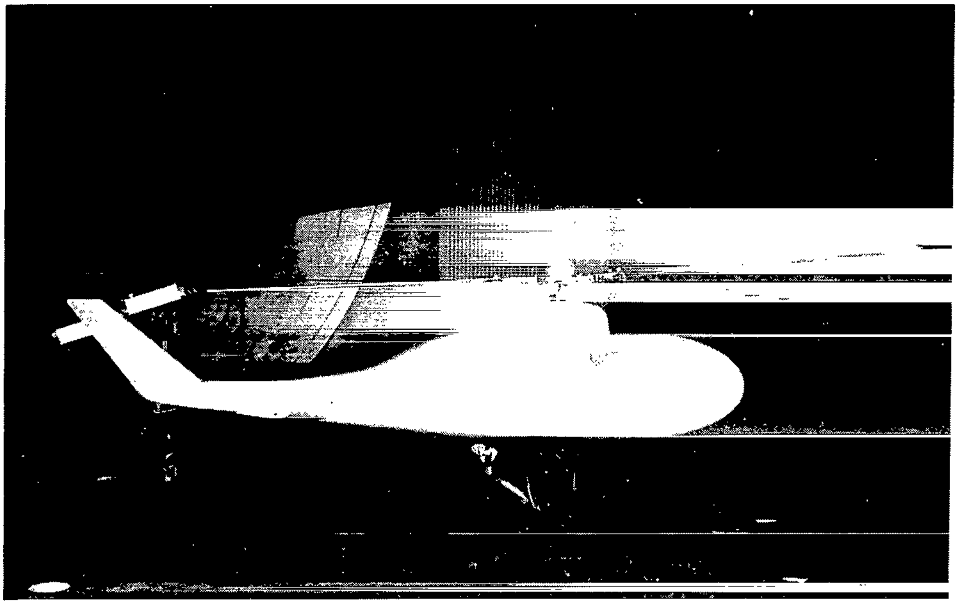

L-69-5337

(a) Side view of model.

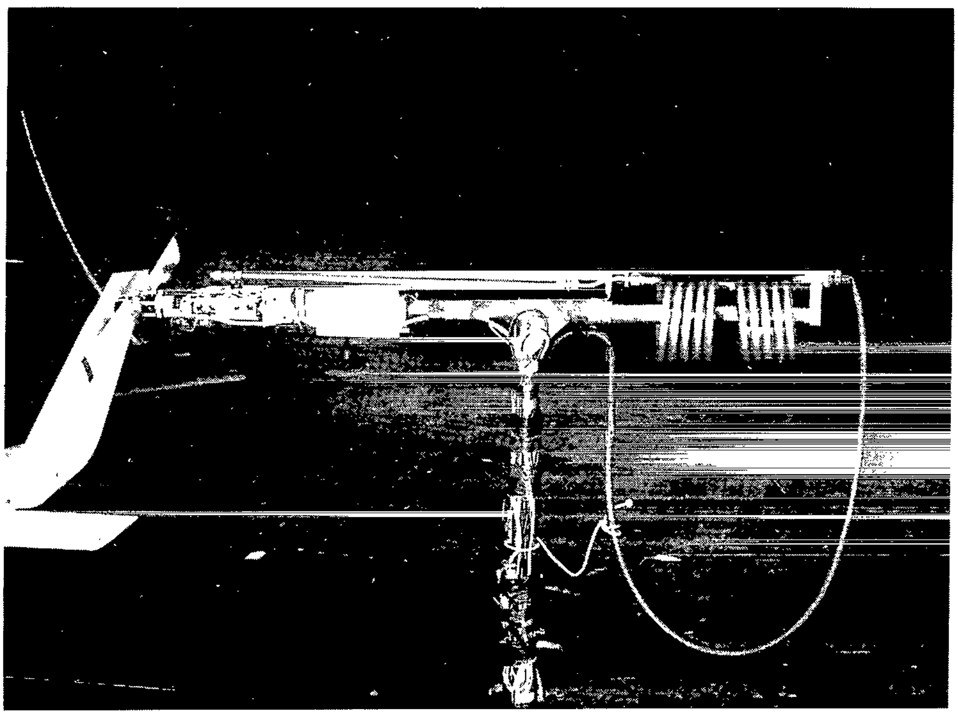

L-69-5336

(b) Tail-rotor apparatus.

Figure 3.- Model installed in Langley full-scale tunnel.

TABLE I.- ROTOR CHARACTERISTICS

	Main rotor	Tail rotor
Diameter, m (ft)	3.35 (11.0)	0.648 (2.125)
Chord, m (ft)	0.171 (0.56)	0.0730 (2.875)
Solidity	0.0651	0.144
Effective cutout, percent	17	20
Twist, deg	-10	0
Airfoil	9.3% thick	NACA 0015
Nominal tip speed, m/s (ft/sec)	227 (746)	224 (736)

TABLE II.- AIRFOIL SECTION COORDINATES

OF MAIN-ROTOR BLADES

[Between chordwise coordinate 0.39911 and the trailing edge, the airfoil is slab-sided]

x_a/c	$\pm y_a/c$
0	0
.00207	.00681
.00770	.01319
.01170	.01600
.01941	.02030
.02756	.02356
.03881	.02770
.05452	.03185
.07778	.03644
.10889	.04074
.15556	.04474
.23333	.04667
.31111	.04504
.39911	.04059
1.00000	.00104

Test Procedure

Data were obtained at tail-wind speeds of 0, 7.5, 10, 12.5, 15, 20, and 25 knots. At each tunnel speed, data were obtained for a range of tail-rotor collective-pitch settings from 0^{o} to near that for stall. The model was tested through the range of tunnel speeds both with the main rotor stopped and with it operated at 250 newtons/meter^2 (5.25 lb/ft^2) disk loading and at zero angle of attack. Since the air supply to the tail-rotor air motor was not governed, but manually regulated, small variations in tail-rotor speed about the nominal value of 224 meters per second (735 ft/sec) usually occurred.

Data Acquisition

Three independent strain-gage balances and one simple strain-gage bridge were used for data acquisition. The balance locations are defined in figure 1. The vehicle balance sensed the total aerodynamic forces and moments acting on the model with the exception of the tail-rotor forces and moments, which were measured by a second balance. Internal to the model fuselage, a separate three-component balance sensed the vertical-fin side force, rolling moments, and yawing moments. A strain-gage bridge on the main-rotor shaft sensed the main-rotor torque.

Simultaneous data signals were recorded for each test condition on a digital data acquisition system. Data recorded included the forces and moments from the three strain-gage balances, the instantaneous rotational speeds of the two rotors, the main-rotor torque, the collective-pitch settings of both rotors, the tunnel velocity, and the air pressure in the supply line to the tail-rotor air motor. The signals from the three strain-gage balances were filtered, and the data recorded were essentially the steady-state values. A correction was applied to the tail-rotor balance measurements to account for a small tare produced by the air line spanning the tail-rotor balance. The largest correction was a 5 percent decrease in the tail-rotor thrust measurement.

Tunnel-Boundary Corrections

No tunnel-boundary corrections were applied to the data, since the objective of the test was to obtain results representative of "in-ground-effect flight." The theoretical results of reference 4 indicate that for the conditions of this investigation, the flow in the tunnel will differ little from that of in-ground-effect flight since the model span to tunnel width ratio (0.26) is modest (based on a ground board width of 13.0 meters (42.5 feet)). The boundary layer on the ground board may have had a measurable effect on the test results but no method was available for correction. The leading edge of the ground board (the point at which the boundary layer begins to build up) was approximately 5.5 meters (18 feet) upstream of the tail rotor.

PRESENTATION OF RESULTS

The basic data of this paper are contained in an appendix. The figures used for discussion of the results were obtained by cross-plotting the basic data at various levels of tail rotor thrust. Since the tail-rotor thrust required to balance the vehicle torque varies with airspeed, most of the data were cross-plotted at various levels of a constant ratio of tail-rotor thrust to vehicle torque. This ratio is presented as the nondimensional torque balance coefficient C_σ. A value of the torque balance coefficient of 1 is equivalent to a flight condition that is trimmed in yaw. A value of this coefficient less than 1 represents a torque unbalance where an unrestrained vehicle would accelerate in a nose-right direction; a value of the coefficient greater than 1 represents a torque unbalance where an unrestrained vehicle would accelerate in a nose-left direction.

The order of presentation of the data in this paper is as follows:

	Figure
Main rotor torque required	4
Tail rotor characteristics – constant C_σ values	5 to 7
Fin force characteristics – constant C_σ values	8 to 10
Wake characteristics	11 to 12
Tail rotor characteristics – constant $C_{T,tr}$ values	13, 14
Fin force characteristics – constant $C_{T,tr}$ values	15
Aerodynamic characteristics of model with main rotor wake (basic data)	16
Aerodynamic characteristics of model without main rotor wake (basic data) . . .	17

Data presented in figures 5 to 8 and 10 include a small extrapolation of the basic data wherein the actual value of the ordinate is at least as large as shown. The extrapolations are indicated by dashed lines.

DISCUSSION OF RESULTS

The results of this investigation with a helicopter model in rearward flight in ground effect indicate that the flight problem of inadequate directional control can be simulated in a tunnel test; further, the results identify three major factors that can cause a reduction in directional-control capability. The three factors are:

(1) An adverse effect of the main-rotor wake on the tail-rotor performance.

(2) An adverse effect of the main-rotor wake on the vertical-fin side force.

(3) An increased level of main-rotor power required over a small range of airspeeds while in ground effect.

The first factor reduces the thrust obtained at a given collective pitch and increases the power required to produce that thrust. The last two factors increase the need for tail-rotor thrust to maintain a heading. All three factors contribute to the requirement for high tail-rotor collective pitch and high tail-rotor power in certain regions of low-speed rearward flight. In the most adverse test condition, the total effect of the three factors is to require tail-rotor collective-pitch settings that would produce twice the tail-rotor thrust required to trim main-rotor torque if losses due to the fin and main-rotor wake were absent.

Vehicle Torque

The tail-rotor thrust required to maintain yaw-trimmed flight is principally that required to balance the main-rotor torque and yawing moments produced by the fuselage and fin. Since the aerodynamics of the fin and the tail rotor are affected by the same phenomenon, fin characteristics are discussed in a subsequent section with those of the tail rotor.

Main-rotor torque requirement.- The variation of the main-rotor torque with airspeed was found to result in approximately a 10-percent increase in the required tail-rotor thrust in the most adverse conditions. The variation of the main-rotor torque with airspeed (fig. 4) indicates that the peak tail-rotor thrust requirement, due to the main-rotor torque, occurs in the 10- to 15-knot airspeed range. This increase in main-rotor power required, for small increases in airspeed from the hover condition, is in agreement with the predicted variation of the ground effect with airspeed (ref. 5). There was no consistent trend of main-rotor torque with variations in the torque-balance factor; thus, the known influence of the tail-rotor wake on the main-rotor wake (ref. 6) was not sufficient, in this case, to cause a measurable effect.

Body yawing moments.- The possibility of adverse body yawing moments cannot be discounted as a significant factor contributing to an increase in tail-rotor thrust requirements. In this investigation, the adverse body moments were obtained, rather inaccurately, from the total vehicle yawing moment $\left(Q_b = Q_v - Q_{mr} - Fl_t - Fx_{cp}\right)$ and were found to vary with airspeed and tail-rotor thrust from essentially zero in hover to approximately 10 percent of the main-rotor torque at 25 knots. Since, even in a pure tail wind, a circular-body fuselage contributes a significant adverse yawing-moment increment to

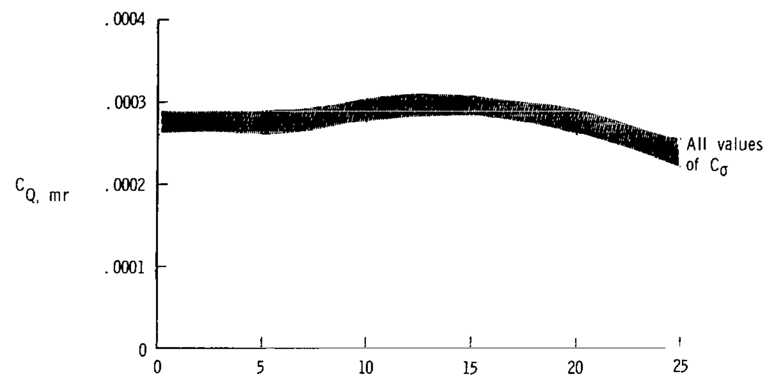

Figure 4.- Main-rotor torque coefficient required. $C_L' = 0.0042$; $\psi = 180^\circ$.

be balanced by the tail rotor, it appears that other more irregular vehicles may have even more significant adverse fuselage yawing moments at rearward velocities involving large yaw angles.

Tail-Rotor and Fin Characteristics

Tail-rotor collective pitch required.- The variation of tail-rotor collective pitch, with rearward velocity, is presented in figure 5. The tail-rotor collective-pitch requirement increases with an increase in rearward velocity until a peak is reached at approximately 12 knots. A slight further increase in rearward velocity results in a sudden decrease in the required tail-rotor collective pitch at 15 knots. The unusual character of the tail-rotor collective-pitch requirement for trimmed flight had been previously noted in unpublished flight-test data. The data were obtained from a helicopter operating at the same disk loading and same relative ground clearance as used in this test. The airspeed at which the abrupt change in collective pitch occurs, in both the flight test and the present wind-tunnel investigation, is near 12 knots.

The similarity of results from a wind-tunnel investigation with flight-test results indicates that at least some of the phenomena that affects tail-rotor performance had been simulated in the wind-tunnel investigation. The flight-test data were restricted to measurements of pedal position, a direct measure of the tail-rotor collective pitch. The measured tail-rotor thrust, torque, fin force, and center-of-pressure data from the wind-tunnel investigation should be typical of the flight-test conditions.

Tail-rotor thrust and torque required.- The tail-rotor thrust and torque requirements (figs. 6 and 7) have the same general character as the collective-pitch requirement.

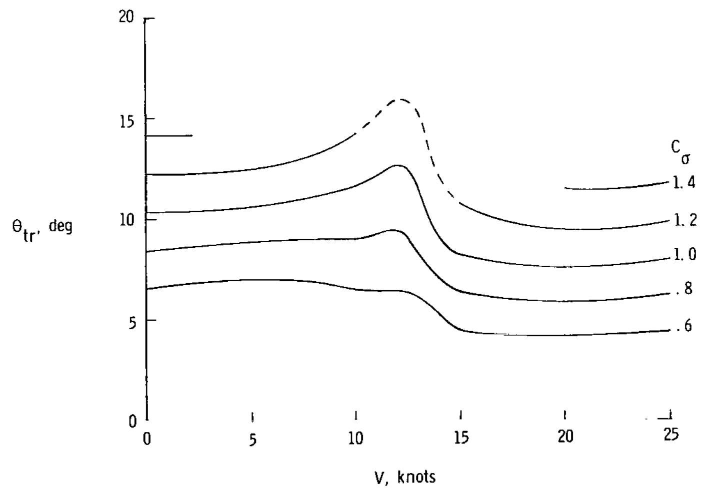

Figure 5.- Tail-rotor collective pitch required. $C_L' = 0.0042$; $\psi = 180^o$. Dashed line denotes extrapolation.

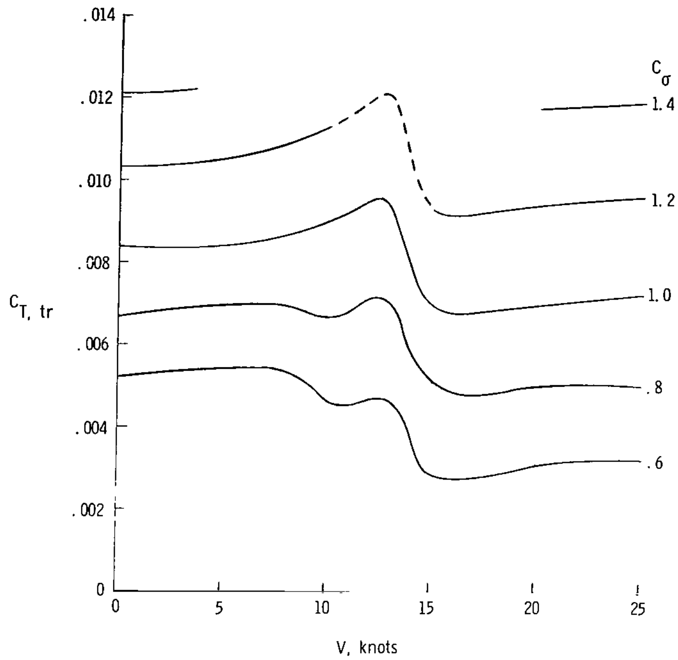

Figure 6.- Tail-rotor thrust coefficient required. $C_L' = 0.0042$; $\psi = 180^\circ$. Dashed line denotes extrapolation.

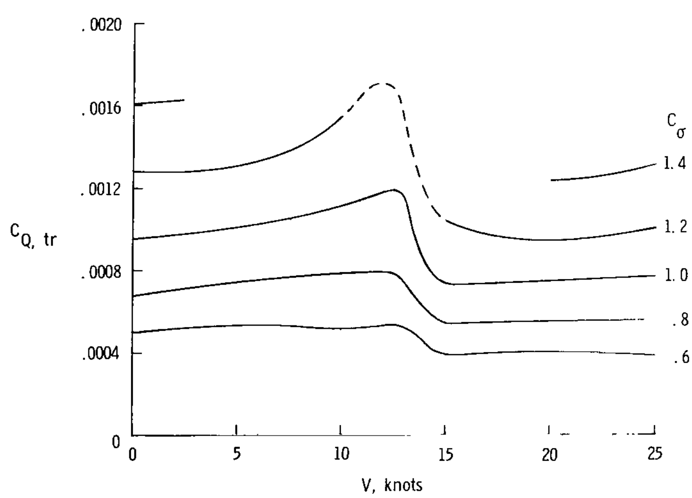

Figure 7.- Tail-rotor torque coefficient required. $C_L' = 0.0042$; $\psi = 180^\circ$. Dashed line denotes extrapolation.

Vertical-fin characteristics.- Several observations can be made from the fin-force data. As shown in figure 8, vertical-fin force is always adverse and has the same general pattern of variation with torque-balance factor and velocity as the collective-pitch-requirement curves.

As indicated in figure 9, the ratio of fin force to tail-rotor thrust is relatively insensitive to torque-balance factor. However, it appears to be highly sensitive to airspeed between 10 and 15 knots, where the fin force decreases from approximately 25 to 14 percent of the tail-rotor thrust. The data indicate that significantly different airflows act on the fin at those two airspeeds.

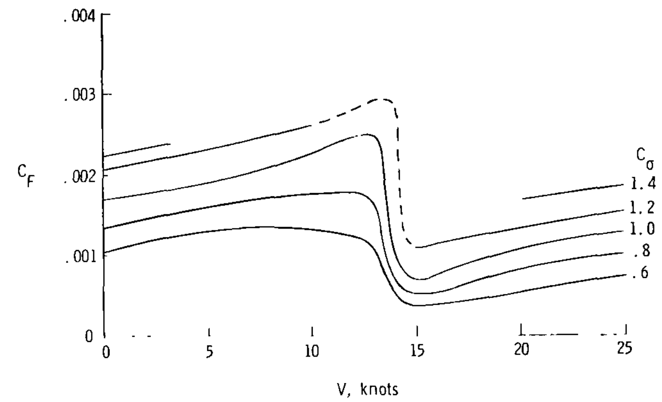

Figure 8.- Fin force coefficient. $C_L' = 0.0042$; $\psi = 180^\circ$. Dashed line denotes extrapolation.

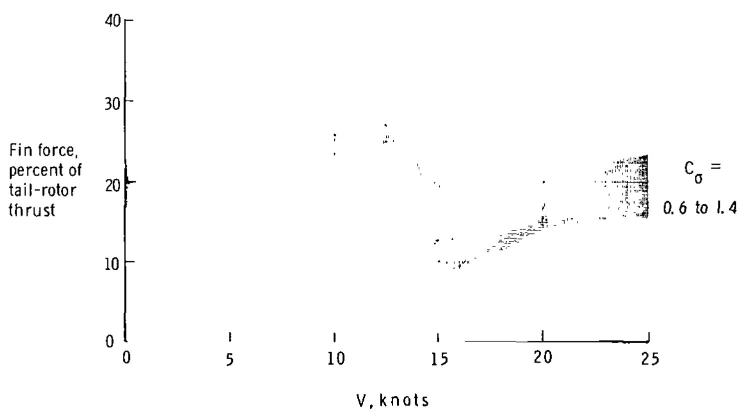

Figure 9.- Fin force as a percentage of tail-rotor thrust. $C_L' = 0.0042$; $\psi = 180^\circ$.

Additional details of the altered airflow are indicated by the center-of-pressure variation with airspeed. (See fig. 10.) The longitudinal position of the fin center of pressure remains constant, that is, near the center of rotation of the tail rotor, with an increase in airspeed, until a velocity of approximately 12 to 15 knots is obtained. As the airspeed increases above 15 knots, the fin center of pressure approaches and passes the fin trailing edge or, more correctly, the leading edge relative to the free-stream flow. This movement of the fin center of pressure with an increase in airspeed is typical of the center-of-pressure movement as the angle of attack is increased on a cambered airfoil from large negative values. (The net flow on the cambered fin does produce a negative angle of attack to the sharp edge of the fin.) The vertical position of the center of pressure, not shown, remains relatively constant at approximately $z_{cp}/R_{tr} = -0.25$.

Ground Vortex Phenomenon

The flow field in which the tail rotor and fin operate is illustrated by the tuft-grid picture of figure 11 taken from reference 7. The tuft grid shows a large ground vortex generated by the interaction of the main-rotor wake and wind in the presence of the ground. The development of this ground vortex is described in references 4 and 8. The inference obtained from comparison of the tuft-grid results of figure 11 with the data in figures 5 to 10 is that in low-speed rearward flight near the ground, the tail rotor is operating within the ground vortex as illustrated by the sketch of figure 12. Therefore, the abrupt change in the measured data occurs when the free-stream flow diminishes the

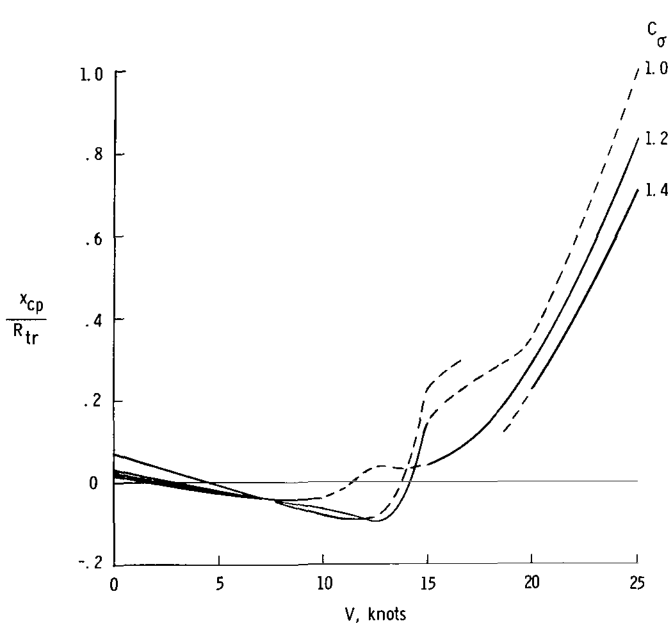

Figure 10.- Fin-force center of pressure. $C_L' = 0.0042$; $\psi = 180^\circ$. Dashed line denotes extrapolation.

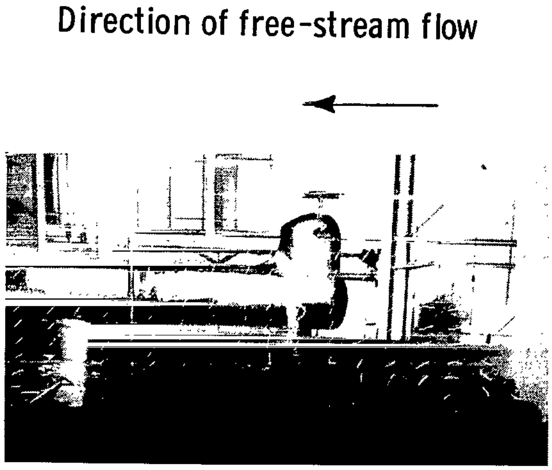

Figure 11.- Tuft grid below rotor. $C_L' = 0.0045$; $V = 9$ knots (from ref. 7).

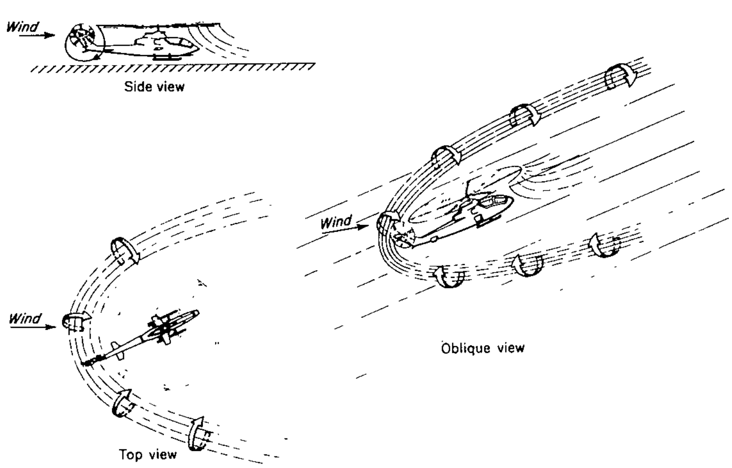

Figure 12.- Sketch of ground-vortex phenomenon.

ground vortex and carries it under the main rotor and away from the tail rotor and fin. Between 10 and 15 knots, the region of the abrupt change in the measured data, the predicted skew angle of the main-rotor wake changes from 30° to nearly 45°. The direction of rotation of the vortex, as determined from examination of figure 11, is in the same direction as the tail rotor of this investigation. In the region where the tail rotor and fin are operating immersed within the ground vortex, the effective angular velocity of the tail rotor may be reduced because of the rotation of the vortex. Therefore, larger tail-rotor collective-pitch settings would be necessary to obtain the required tail-rotor thrust to balance the vehicle yawing moment.

The approach to providing an adequate directional-control capability in rearward flight must be aimed at identifying tail-rotor-fin configurations that minimize the adverse effects of the ground vortex. Two methods of reducing the severity of the problem are suggested by a review of figure 12. First, the direction of tail-rotor rotation could be changed to that preferred for rearward flight: opposite to the direction of rotation of the ground vortex, that is, blades going aft at the top of the disk. A qualification should be noted, however, that if the tail-rotor rotational speed is extremely high, rotation against the ground vortex may result in an increase in tail-rotor power required because of a high Mach number drag divergence. Second, a review of the figure suggests that an increase in tail-rotor height relative to the main-rotor disk could lessen the effects of the vortex.

The presence of a ground vortex adjacent to the upwind side of the main rotor suggests that the problem of adverse wake effects on the fin and tail-rotor performance may extend, to some degree, throughout the yaw-angle range from 90° to 270°. The data included in this report ($\psi = 180^{\circ}$) certainly do not represent the worst case and, in fact, the directional-control limit noted on the AH-1G, for instance, occurs in a left-rear-quartering tail wind (ref. 1). The case of a left-rear-quartering tail wind may be one of extreme flow unsteadiness for the tail rotor which is approaching the vortex-ring state.

The presence of both a tail-rotor vortex-ring state and a ground vortex will result in conditions where the unsteadiness of the flow would make it extremely difficult for the pilots to maintain directional control in a region that is already directionally unstable. An additional factor, pointed out in references 4 and 8, is that the ground-vortex phenomenon can involve hysteresis; that is, the previous velocity history may define the conditions where the adverse effects of the ground vortex are encountered. Pilot-control actions, variable aircraft height, and unsteady winds would contribute to the hysteresis effect and would result in a general unsteadiness in the directional control in the critical region of rearward flight. The total effect of these various factors would be to cause overcontrolling of the tail-rotor collective pitch by the pilot and would result in potentially damaging power surges to the tail-rotor drive mechanism.

Effect of Main-Rotor Wake on Tail-Rotor-Fin Performance

The influence of the ground vortex on the tail rotor and fin may be partially isolated by comparison of their performance with and without the main-rotor wake.

The effect of the main-rotor wake, as shown in figure 13, is to require higher tail-rotor collective pitch settings to maintain constant tail-rotor thrust below approximately 17 knots. At 12 knots, an increase of nearly 20 percent in tail-rotor collective pitch is shown to be required. Any increase in density attitude would adversely affect tail-rotor performance and require the use of even higher blade pitch settings in order to achieve

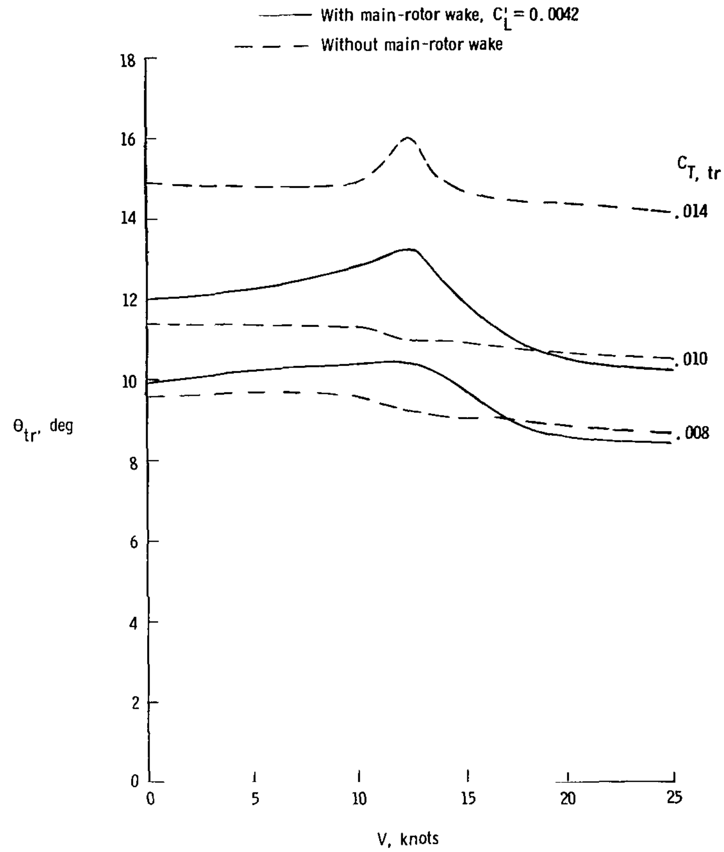

Figure 13.- Effect of main-rotor wake on tail-rotor collective pitch at constant tail-rotor thrust. $\psi = 180^{\circ}$.

directional trim. The hump in the curve for 0.014 tail-rotor thrust coefficient indicates that an anomaly exists in the tail-rotor measurements at high collective-pitch settings for the conditions without the main-rotor wake. The phenomenon associated with the anomalous measurement has not been identified, but it is not considered to be a measurement error. Data at corresponding high collective-pitch settings with the main-rotor wake were not obtained.

As shown in figure 14, the main-rotor wake causes a small increase in the torque requirement at constant tail-rotor thrust. The increased tail-rotor torque requirement is believed to be caused primarily by the ground vortex producing a lower effective rotational speed. The anomaly present in the preceding figure also is present in figure 14.

The main-rotor wake, as shown in figure 15, also causes an increase in the fin force of nearly 100 percent in the rearward velocity range from 0 to 10 knots. At 12 knots the fin force is 25 percent of the tail-rotor thrust. For rearward velocities greater than about 16 to 17 knots, the effect of adding the main-rotor wake is to cause a small decrease in the adverse fin force. The adverse increment in fin force, due to adding the main-rotor

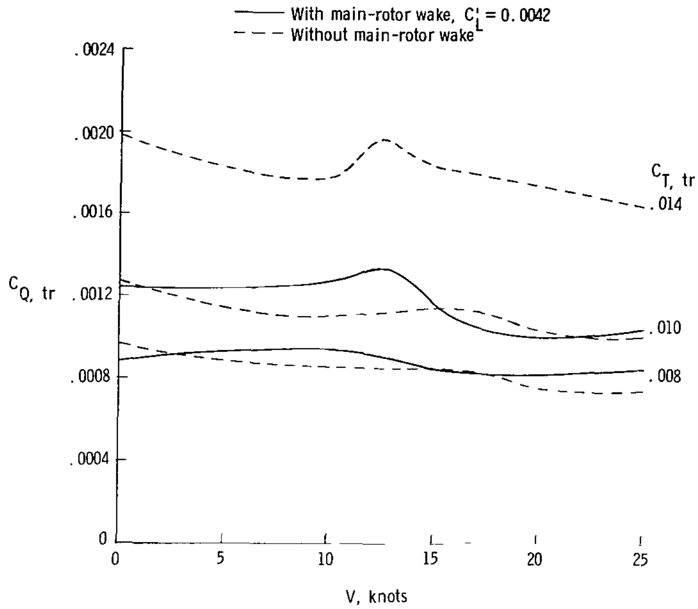

Figure 14.- Effect of main-rotor wake on tail-rotor torque coefficient at constant tail-rotor thrust coefficient. $\psi = 180^{\circ}$.

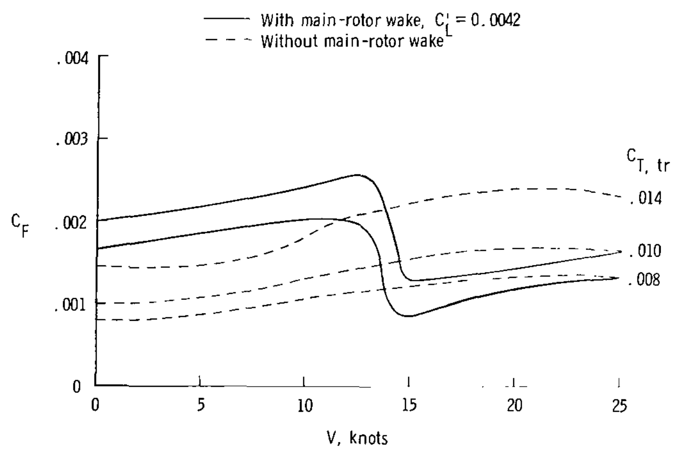

Figure 15.- Effect of main-rotor wake on fin force coefficient at constant tail-rotor thrust coefficient. $\psi = 180^{\circ}$.

wake, changes dramatically between 10 and 15 knots, the region where it is assumed that the ground vortex is removed from the vicinity of the tail rotor and fin by an increase in the free-stream flow.

These adverse effects of the main-rotor wake on the performance of the tail rotor and fin are amplified because of the increase in main-rotor power required in the critical tail-wind range. The 10-percent increase in main-rotor torque requires more than a 10-percent increase in tail-rotor thrust because of the increased adverse fin force. The corresponding increase in tail-rotor torque, because of the ground vortex, is also disproportionately large in the critical condition.

One of the factors previously identified as causing a reduced tail-rotor effectiveness is the size of the vertical fin. (See ref. 6.) The adverse fin force, in hover, has been shown to be directly proportional to the fin size. Efforts at reducing the effects of the main-rotor wake on the fin force are not likely to result in any substantial reduction below the basic fin force occurring without the main-rotor wake. However, without the main-rotor wake, an 85-percent increment in the adverse fin force occurs as a result of an increase in rearward velocity from 0 to 25 knots (fig. 15). This factor emphasizes the value of vertical-fin configurations that provide the smallest possible adverse fin force in a hover.

CONCLUSIONS

An investigation was conducted in the Langley full-scale tunnel to study the aerodynamics that produce directional-control problems for a helicopter with a tail rotor in low-speed rearward flight in ground effect. Based on the data obtained, the following conclusions have been reached:

1. A large ground vortex, generated by the interaction of the main-rotor wake and the wind in the presence of the ground, is a source of large adverse effects on the tail-rotor performance and the vertical fin. At the most critical test condition, the effects seriously decrease the tail-rotor thrust available and increase the adverse fin force to nearly 25 percent of the remaining tail-rotor thrust.

2. A disproportionately larger increase in the required tail-rotor thrust and torque occurs than is dictated by the increase in main-rotor power required at the most critical test condition.

3. The total effect of the adverse fin force, decreased tail-rotor performance, and the increased main-rotor power requirement is to require high tail-rotor collective-pitch settings for the most critical condition. If the adverse effects were absent, the same pitch setting would produce twice the tail-rotor thrust required to trim main-rotor torque.

4. When rearward speed is sufficiently increased, the free-stream flow diminishes the ground vortex and carries it under the main rotor and away from the tail rotor and fin. This condition results in reduced interference and an abrupt change in the tail-rotor collective pitch required with rearward airspeed.

Langley Research Center,
National Aeronautics and Space Administration,
Hampton, Va., February 3, 1971.

APPENDIX

BASIC DATA

Basic data which describe the aerodynamic characteristics of the model with and without the main-rotor wake are given in figures 16 and 17.

Some of the tail rotor and fin data show the effect of unsteady tail-rotor flow at high tail-rotor collective pitch. In these cases, the tail-rotor thrust and torque fluctuated simultaneously with tail-rotor speed; low thrust and torque coefficients correspond to overspeeds of up to 5.3 percent.

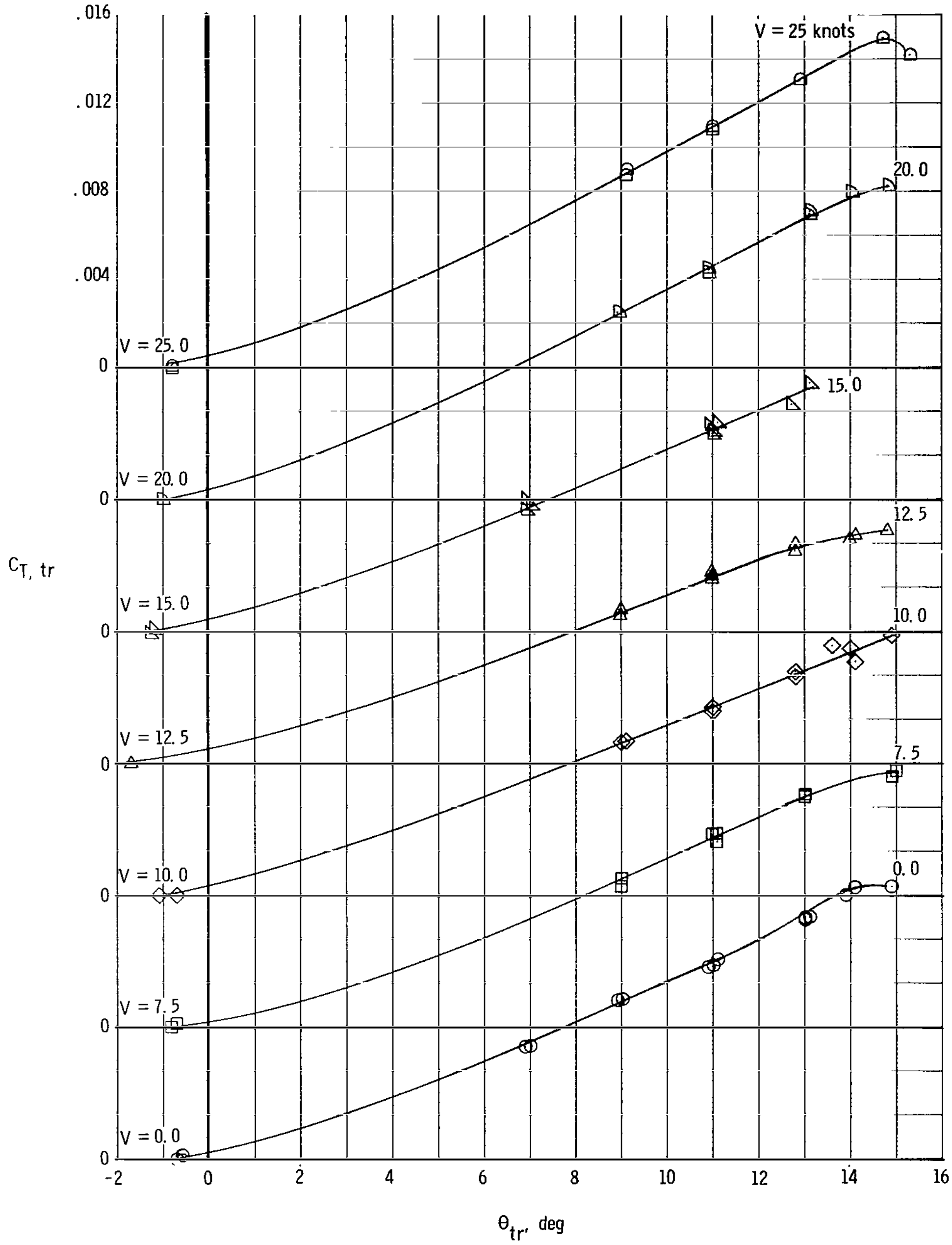

(a) Tail-rotor thrust.

Figure 16.- Aerodynamic characteristics of model with main-rotor wake. $\psi = 180^{\circ}$.

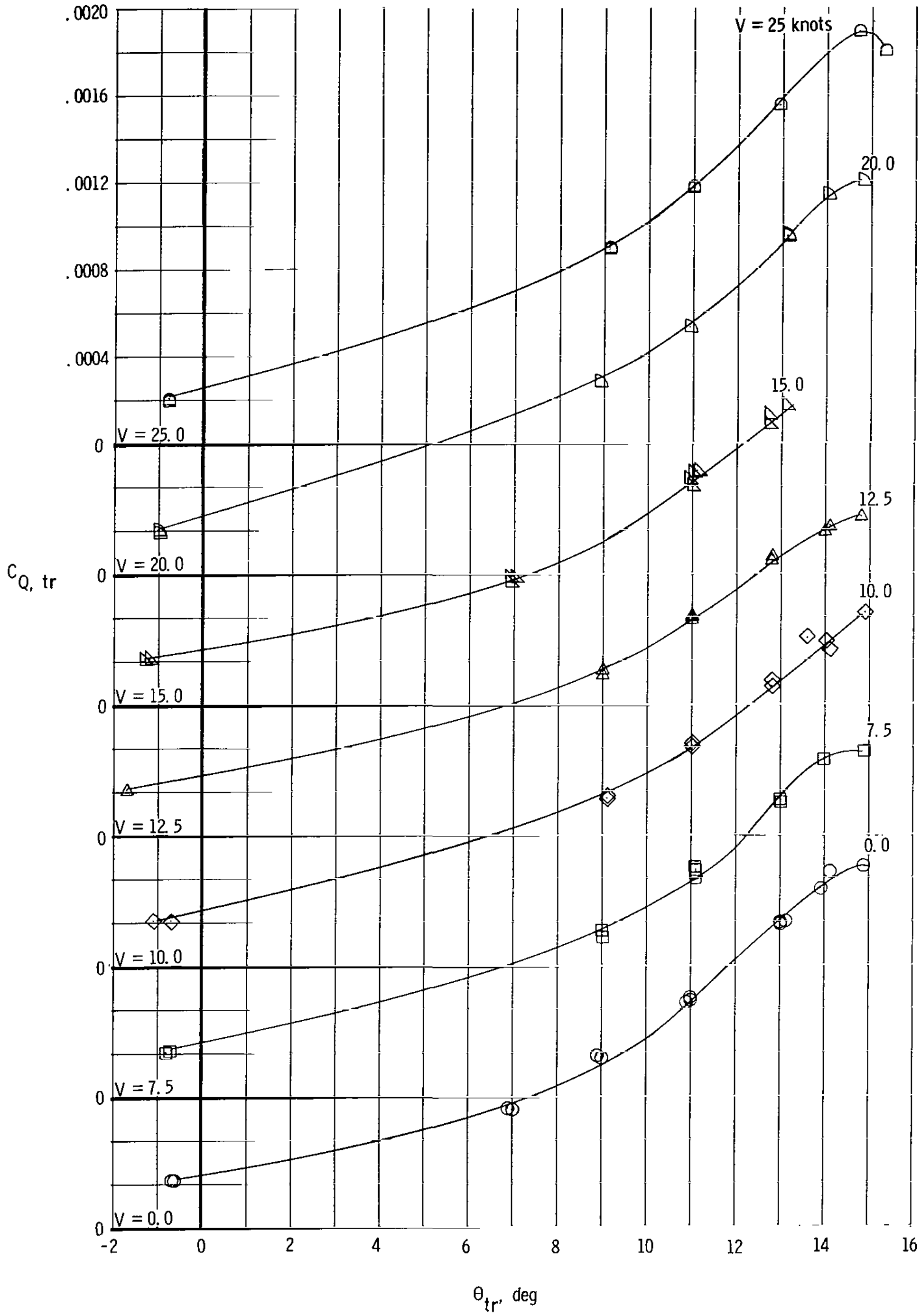

(b) Tail-rotor torque.

Figure 16.- Continued.

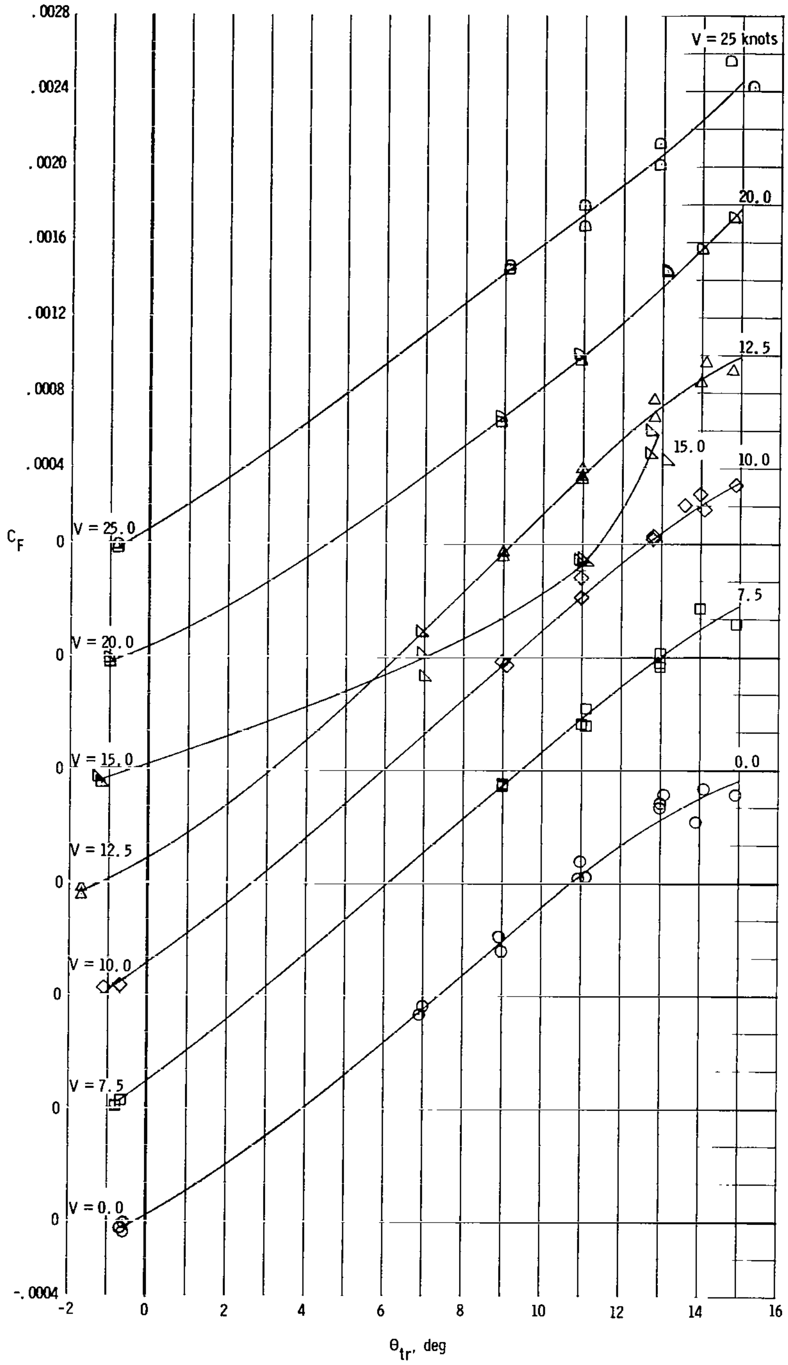

(c) Fin force.

Figure 16.- Continued.

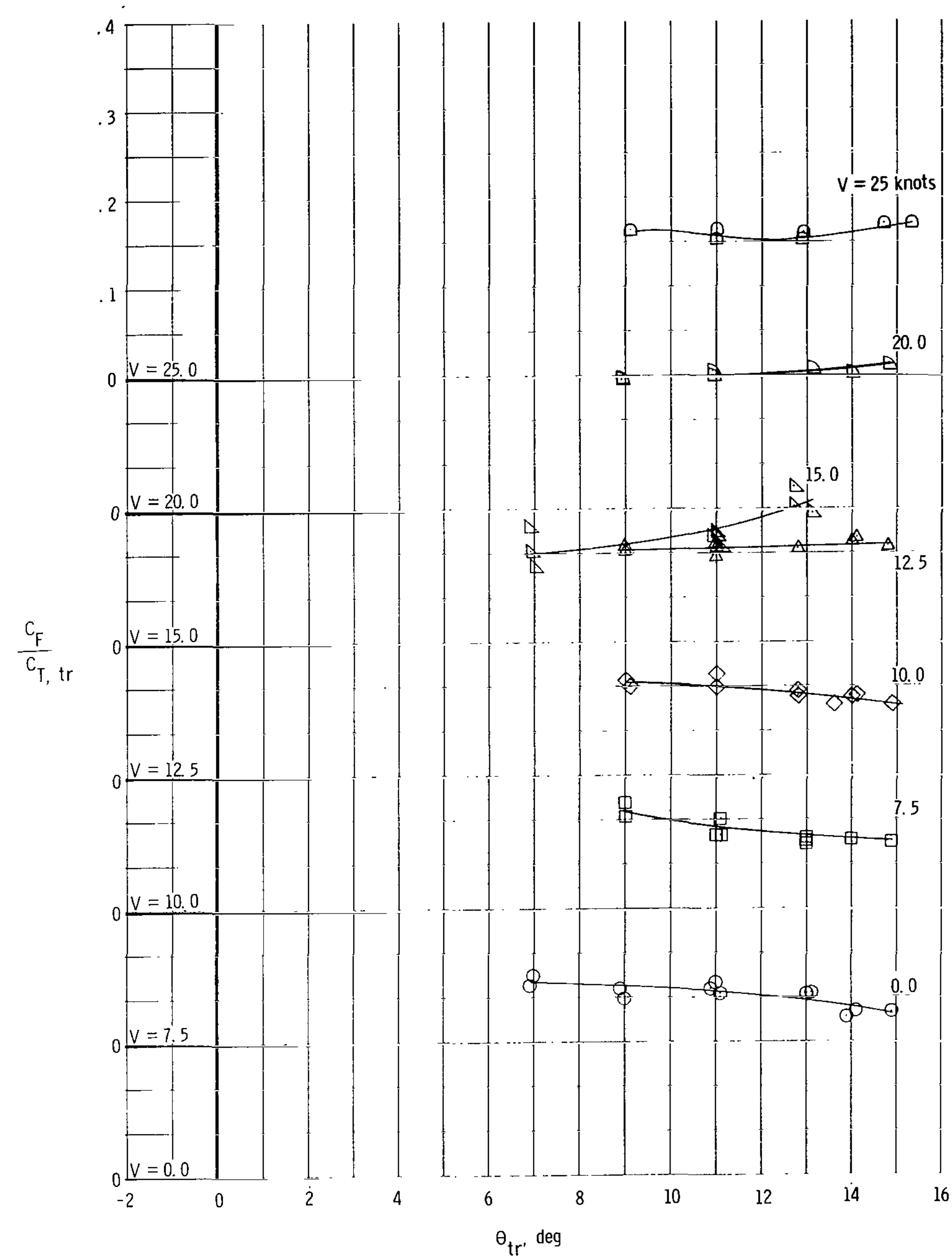

(d) Ratio of fin force to thrust.

Figure 16.- Continued.

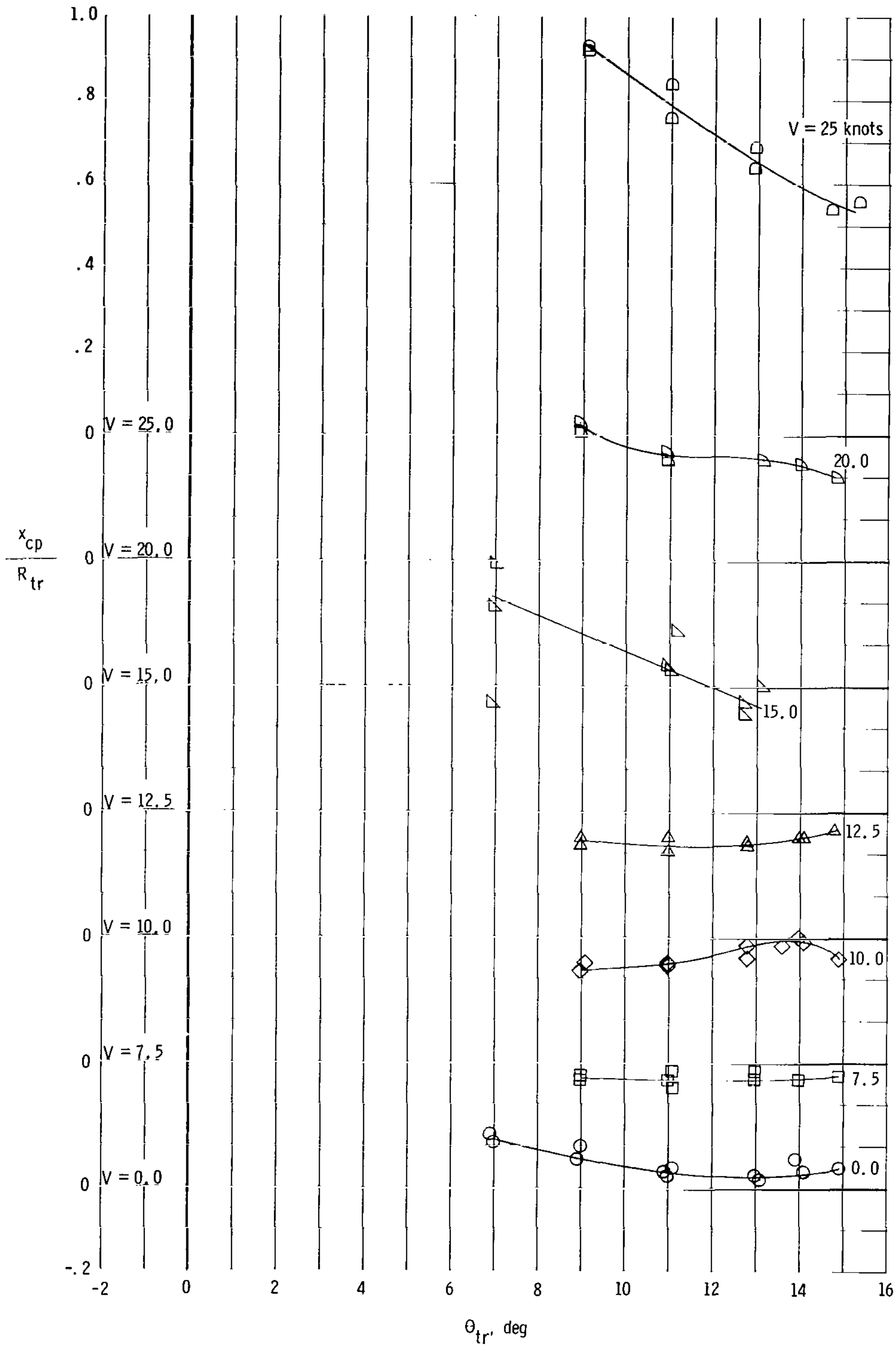

(e) Fin center of pressure.

Figure 16.- Continued.

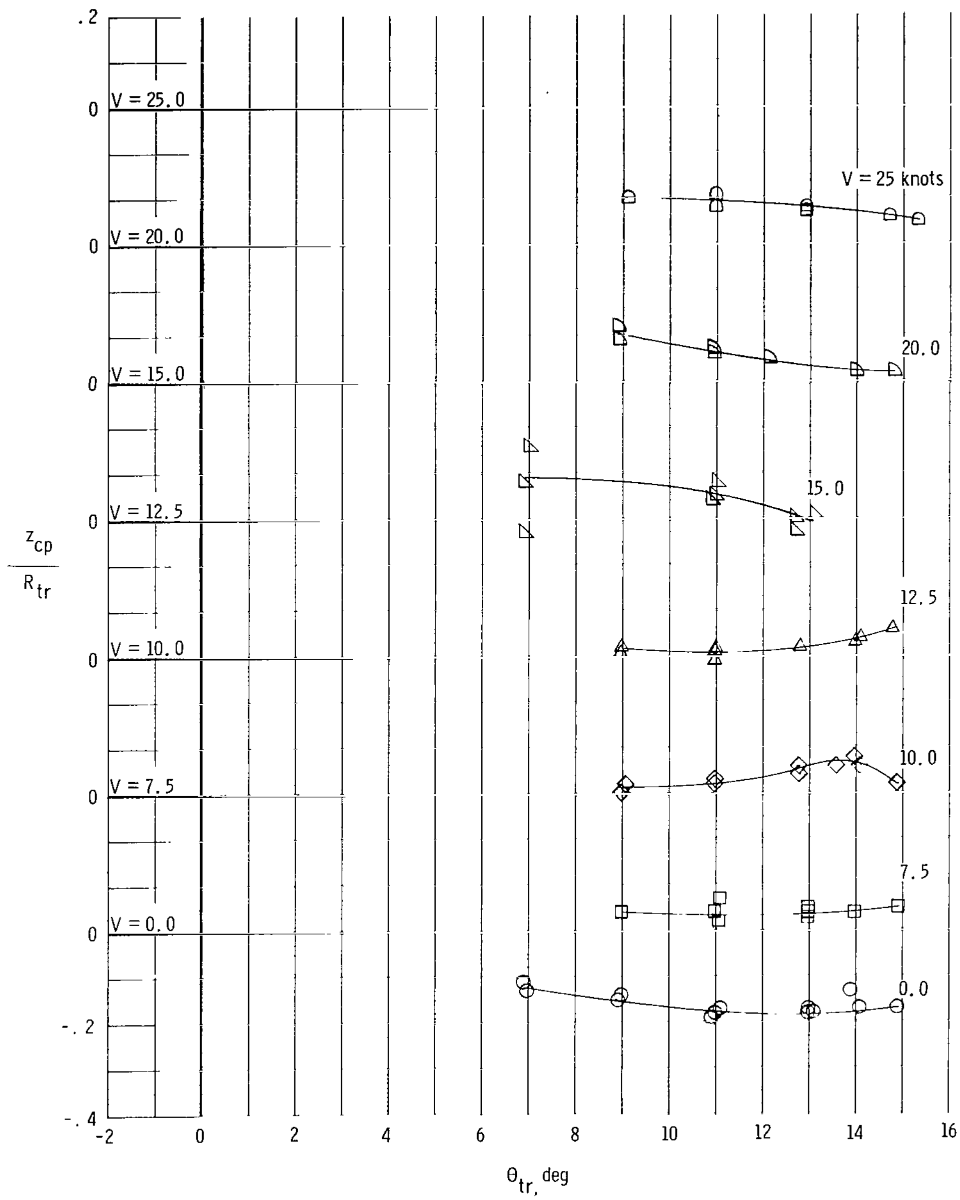

(e) Concluded.

Figure 16.- Continued.

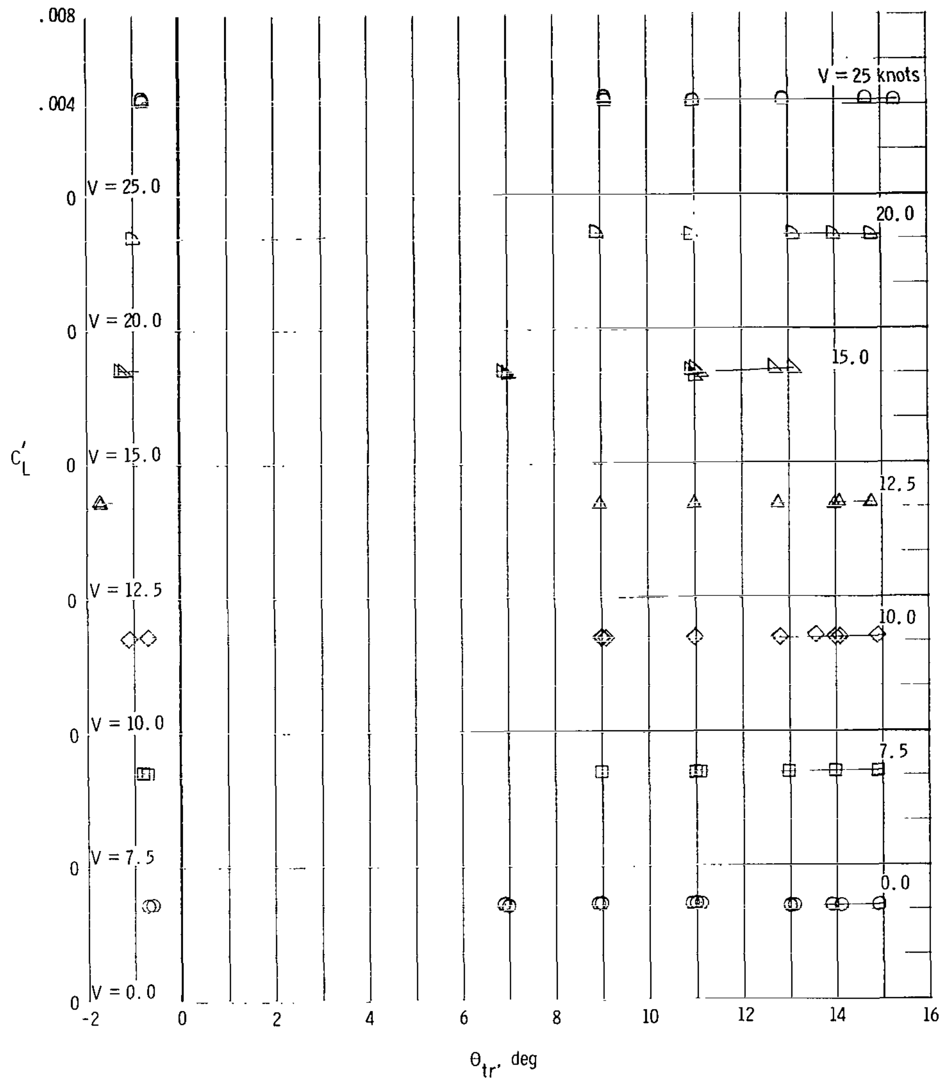

(f) Main-rotor lift.

Figure 16.- Continued.

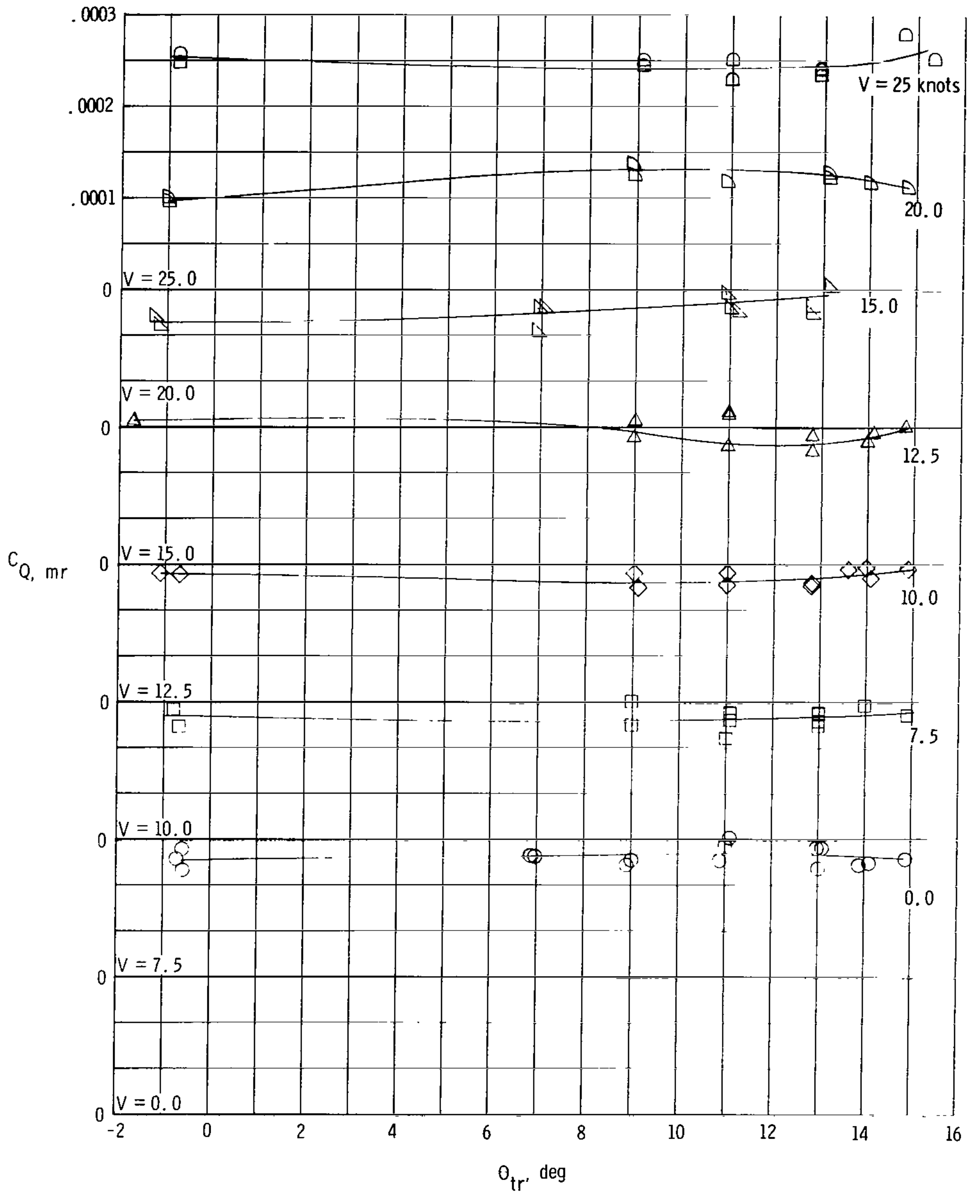

(g) Main-rotor torque.

Figure 16.- Continued.

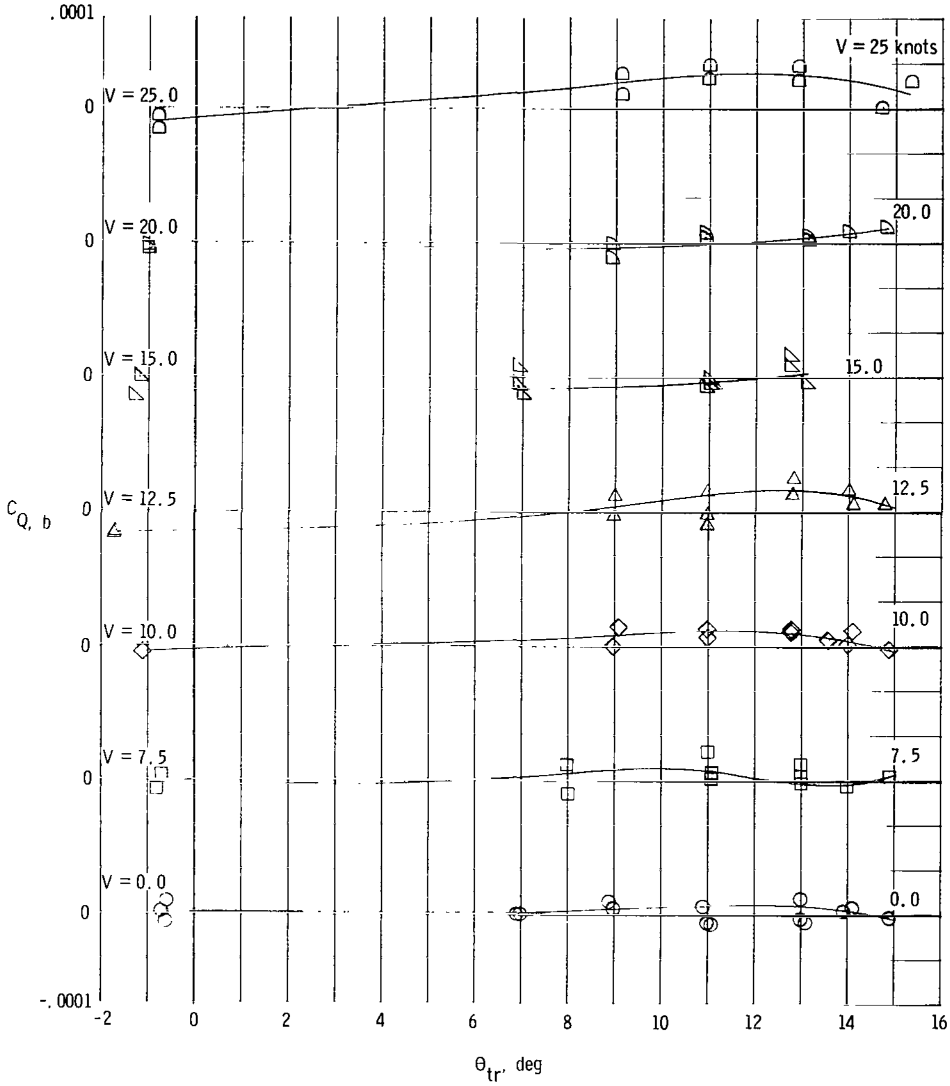

(h) Body torque.

Figure 16.- Continued.

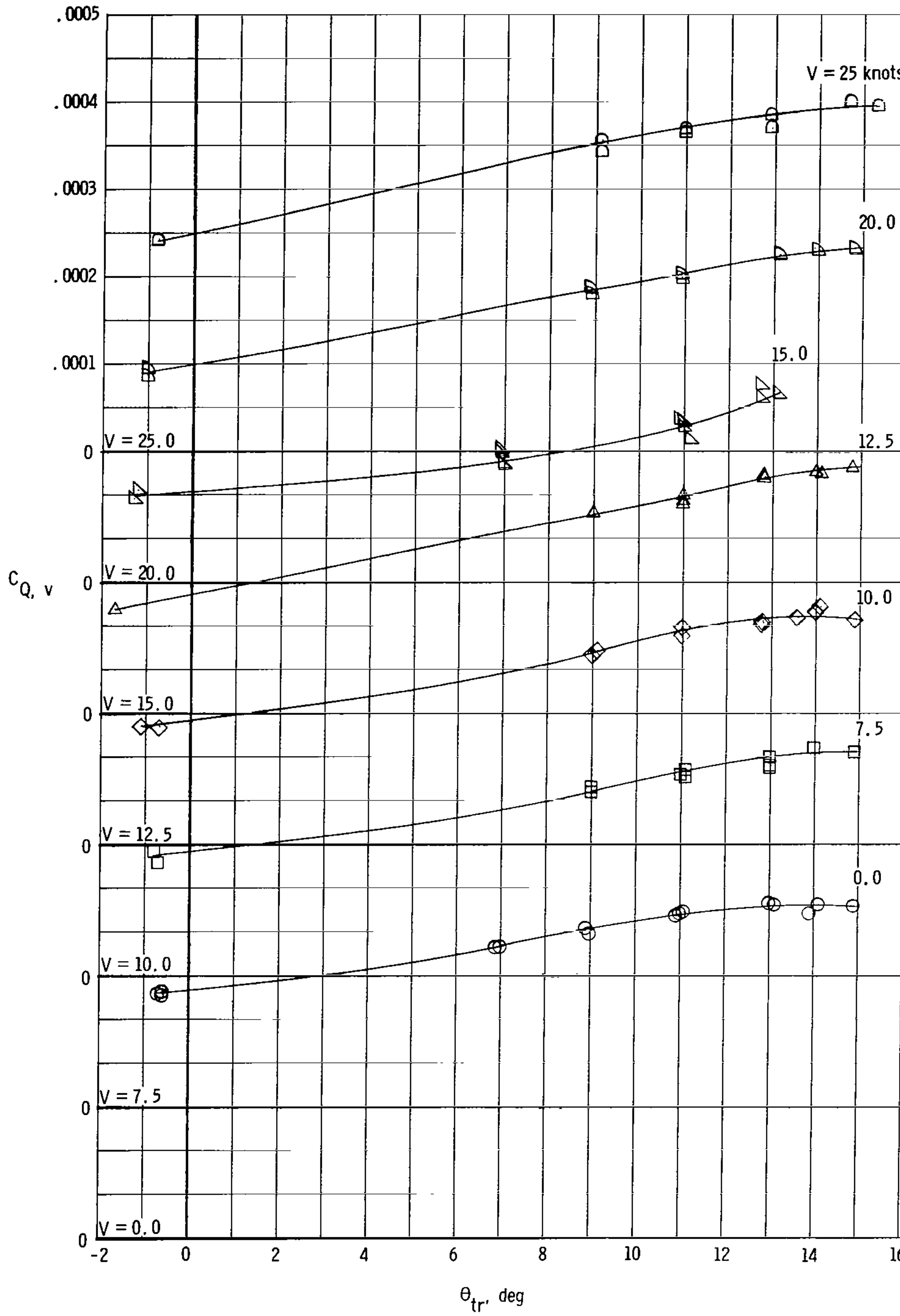

(i) Vehicle torque.

Figure 16.- Continued.

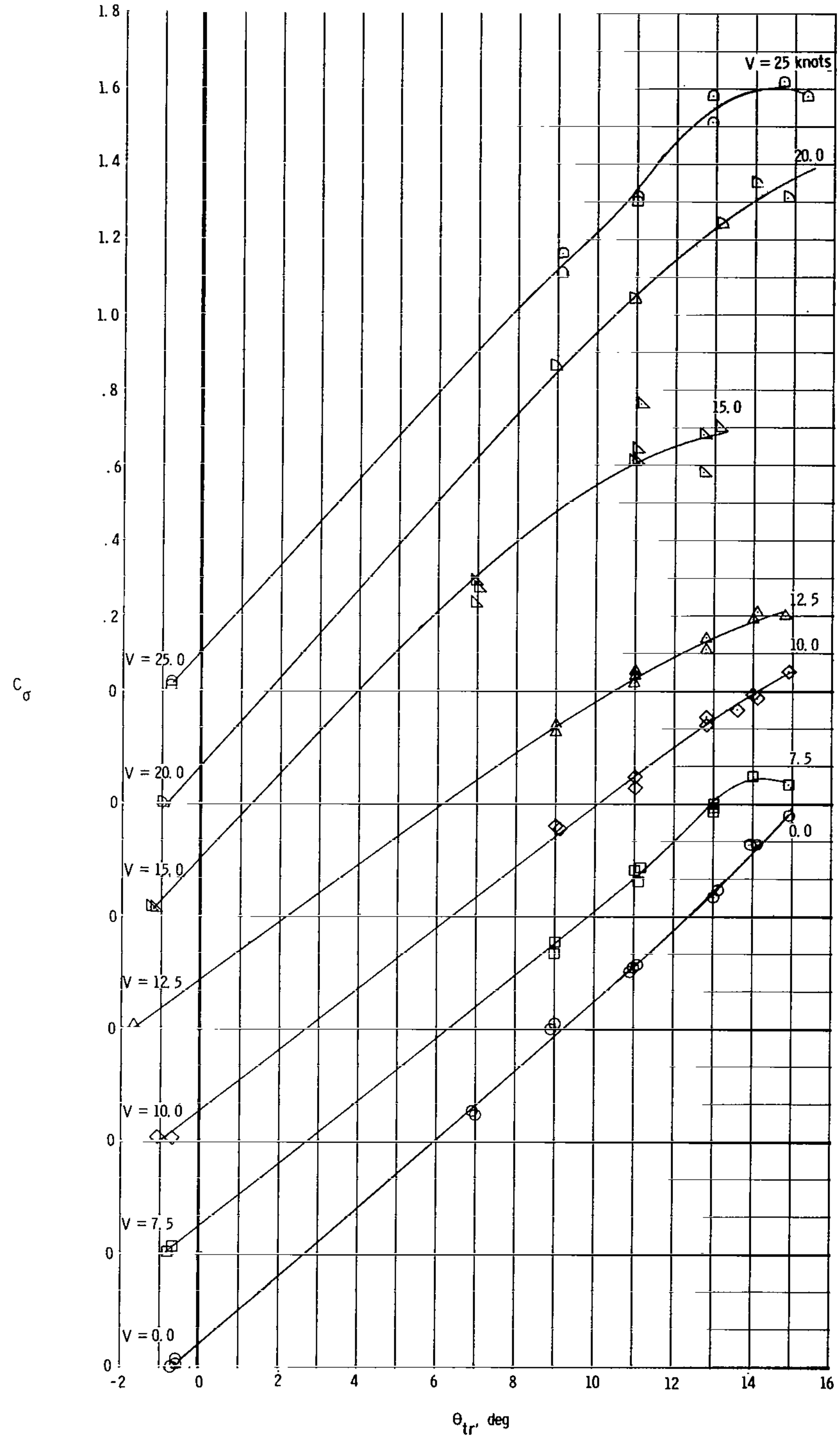

(j) Torque balance factor.

Figure 16.- Concluded.

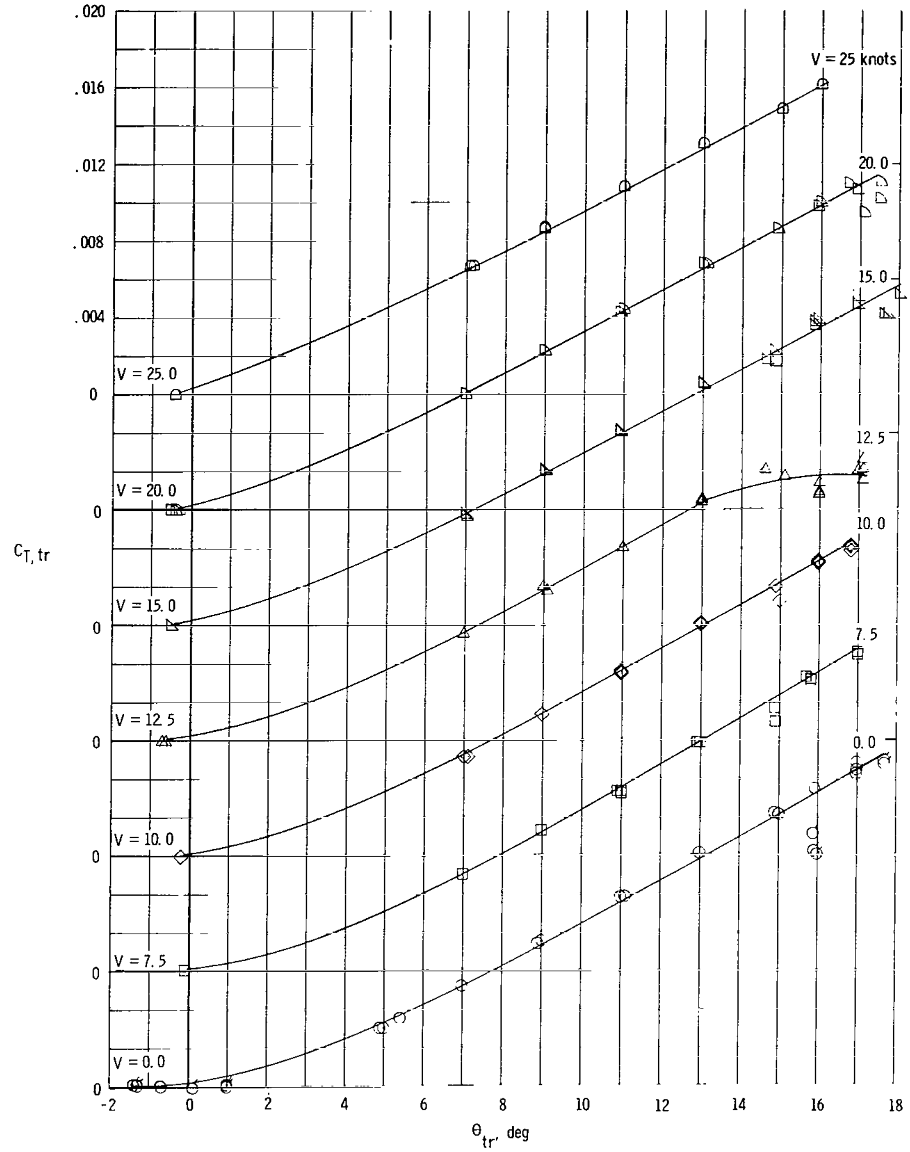

(a) Tail-rotor thrust.

Figure 37.- Aerodynamic characteristics of model without main-rotor wake. $\psi = 180^{\circ}$.

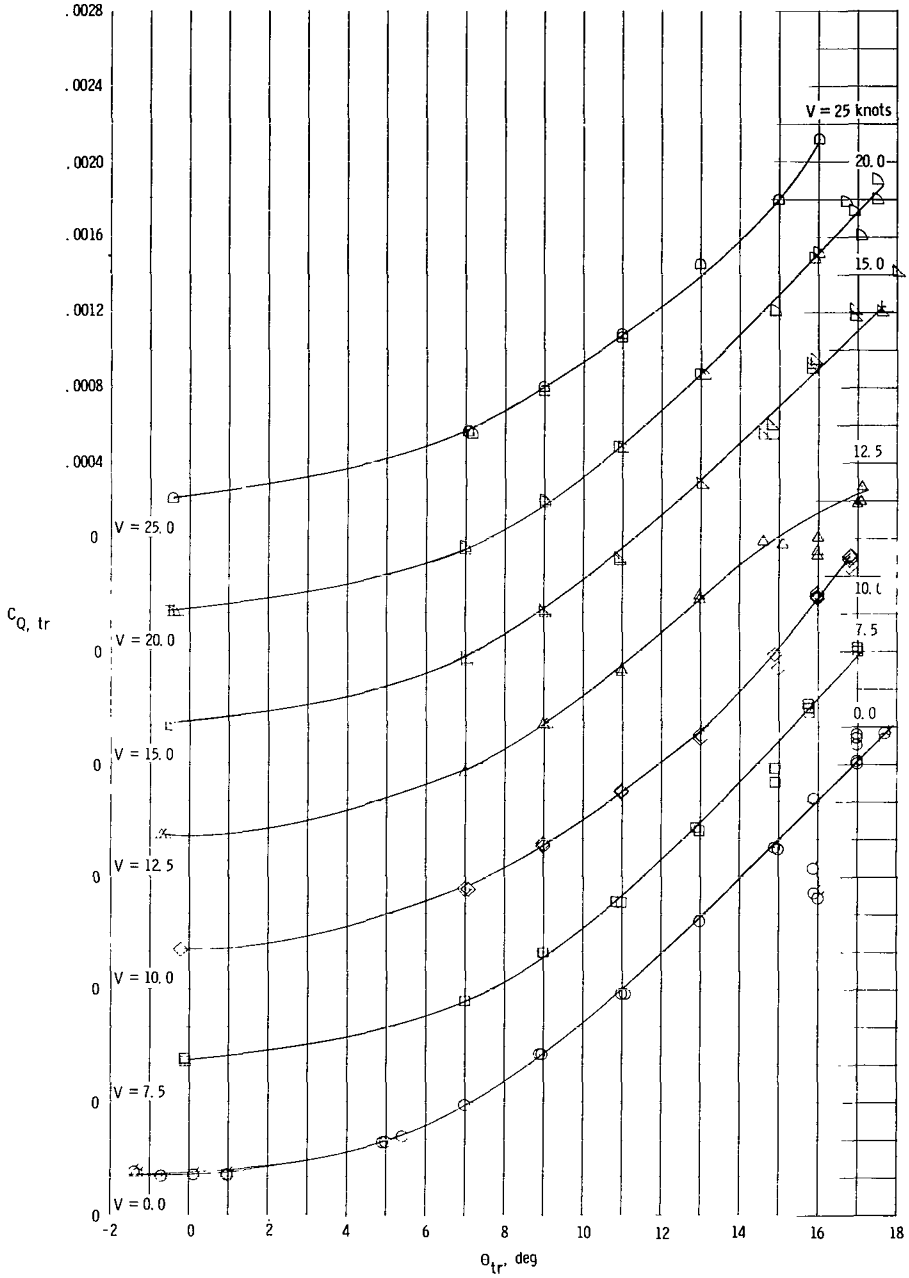

(b) Tail-rotor torque.

Figure 17.- Continued.

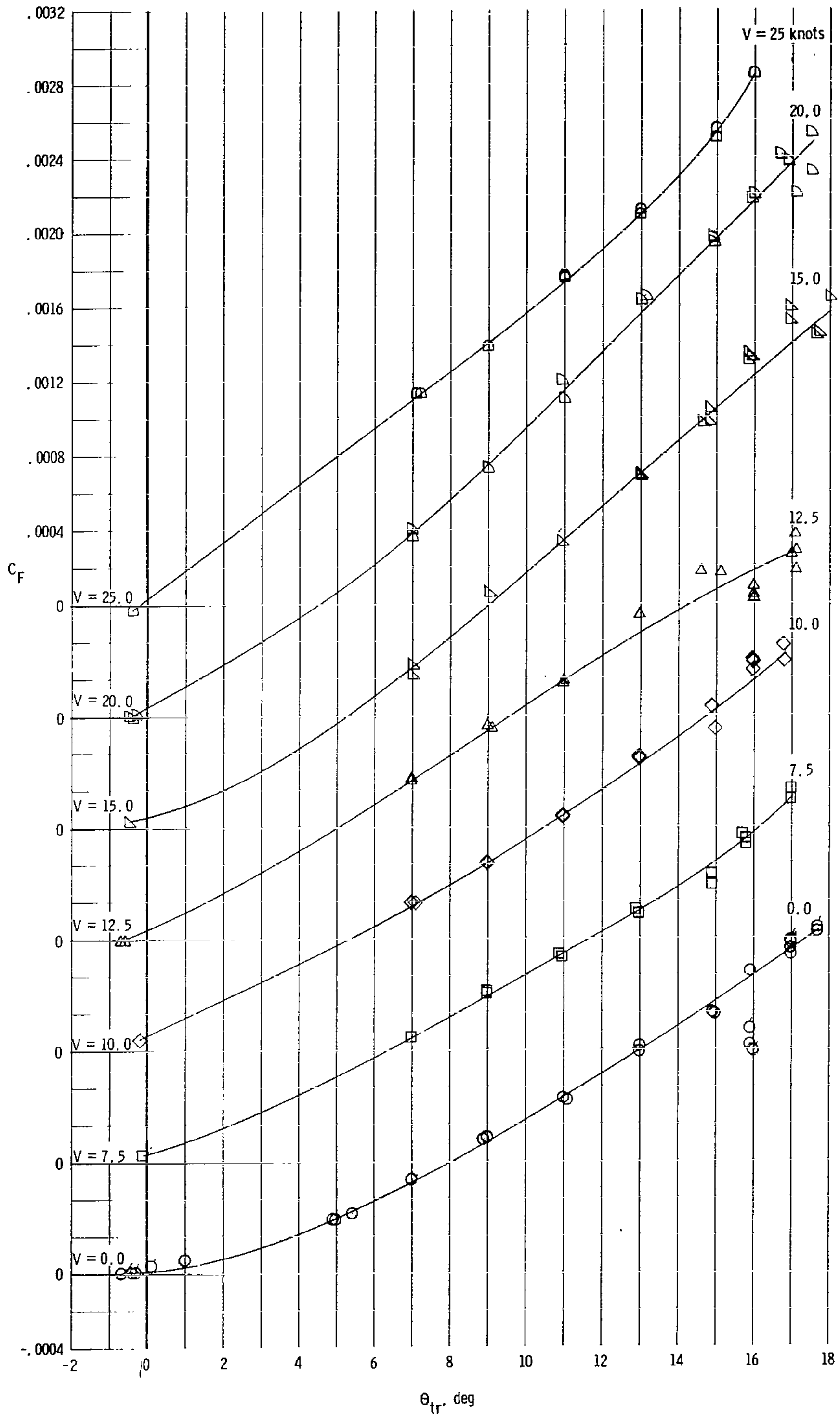

(c) Fin force.

Figure 17.- Continued.

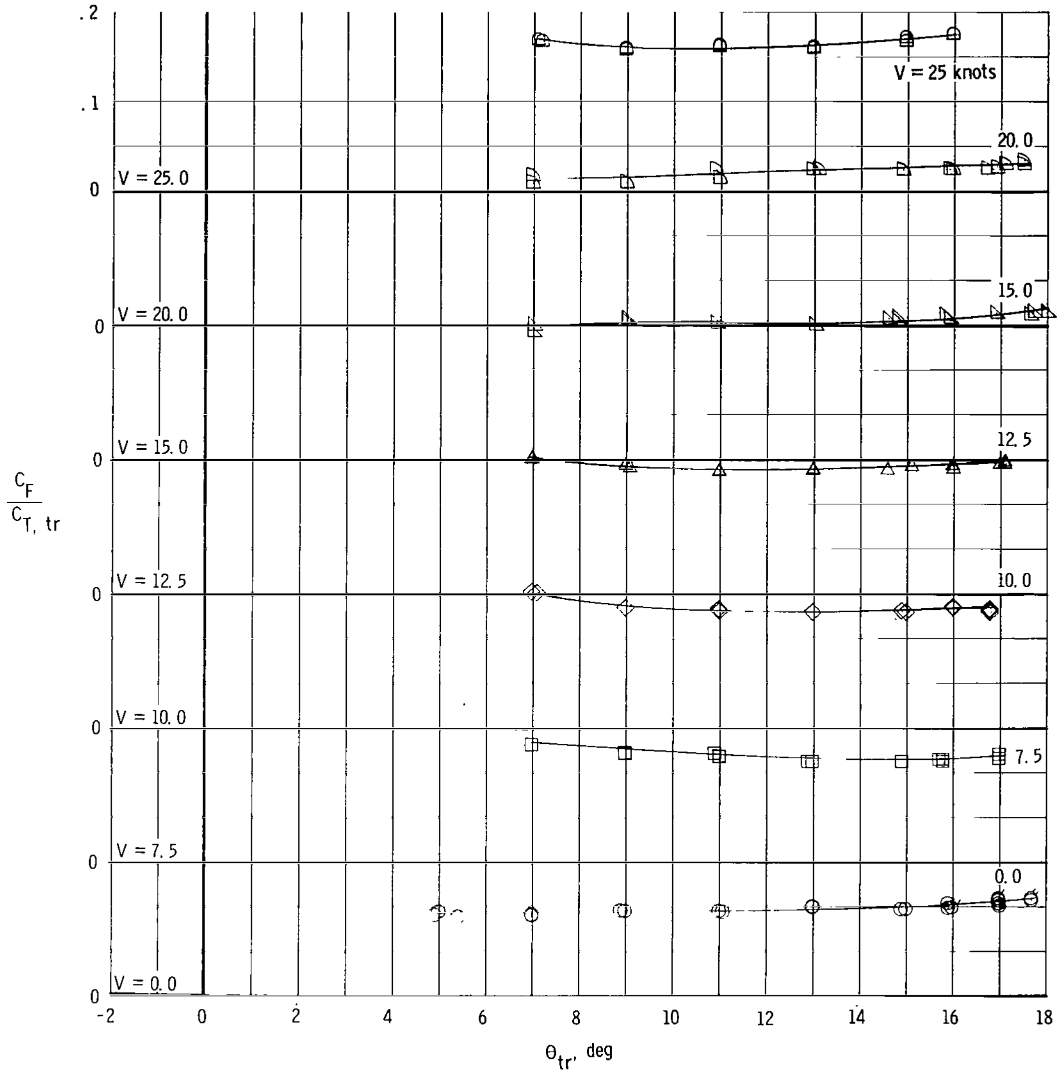

(d) Ratio of fin force to thrust.

Figure 17.- Continued.

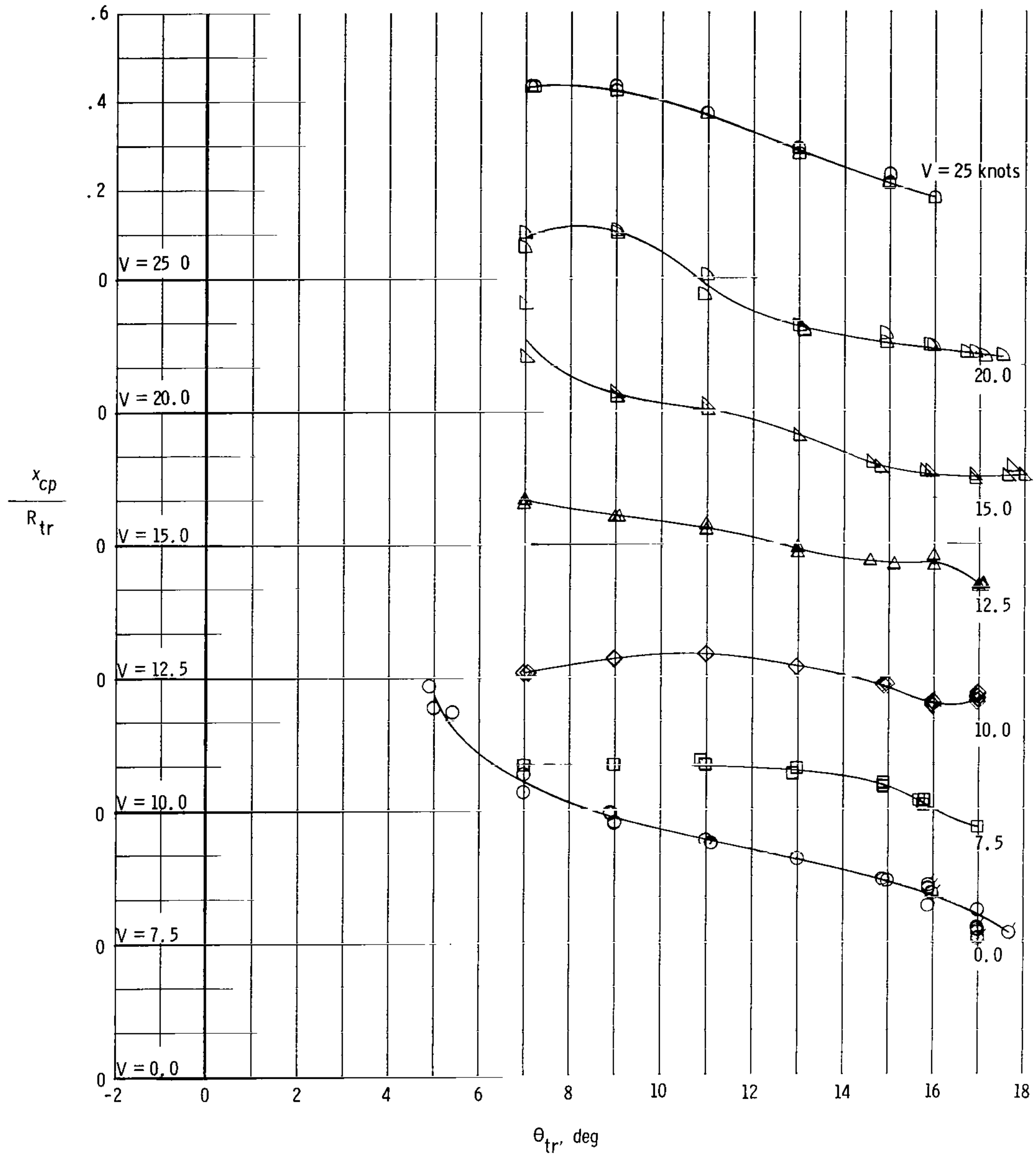

(e) Fin center of pressure.

Figure 17.- Continued.

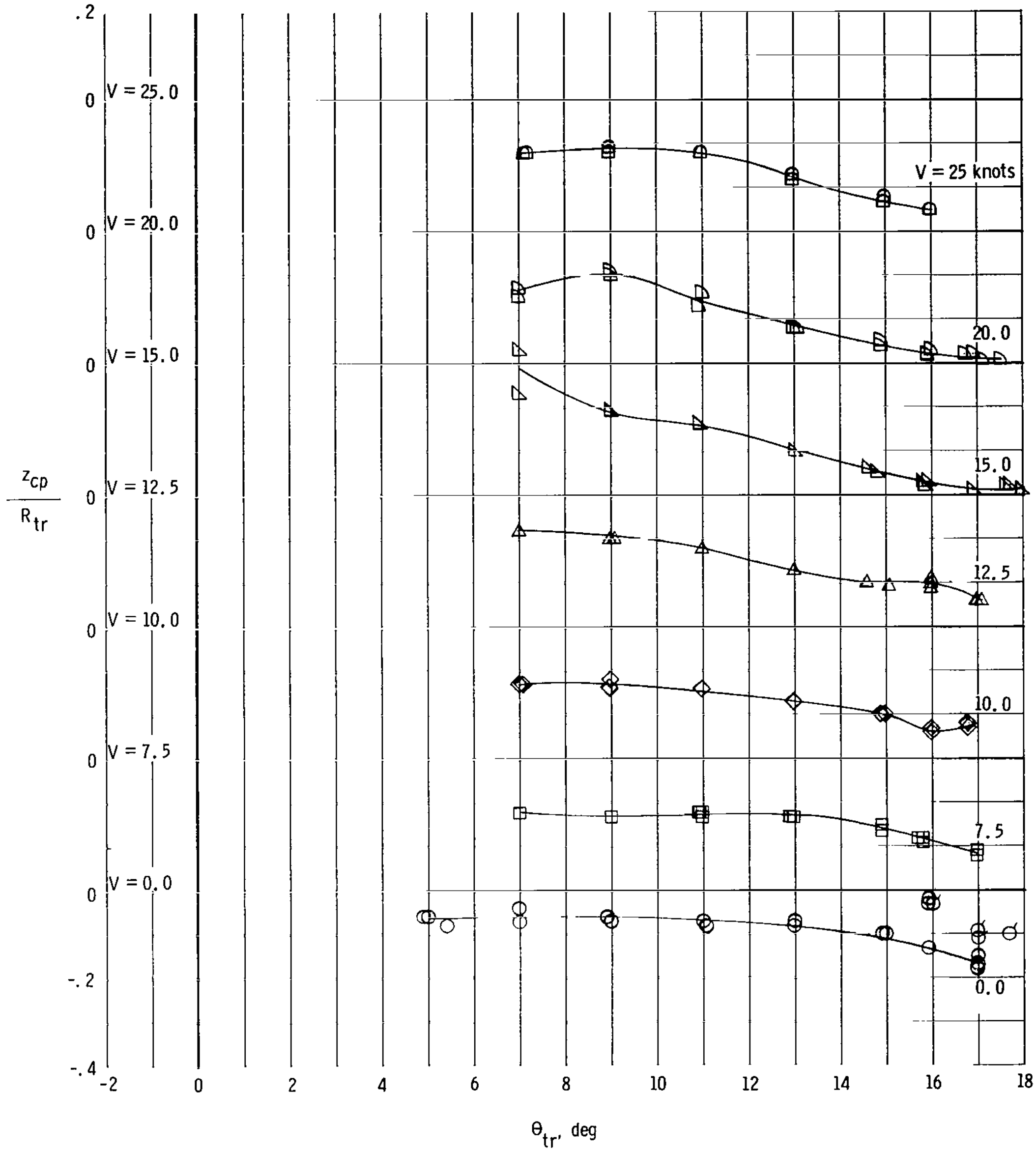

(e) Concluded.

Figure 17.- Concluded.

REFERENCES

1. Connor, William J.: The Huey Cobra in Vietnam. 1968 Report to the Aerospace Profession, Tech. Rev., vol. 9, no. 2, Soc. Exp. Test Pilots, 1968, pp. 25-32.
2. Anon.: Tail Rotor and Yaw Control. Special Feature Issue of J. Amer. Helicopter Soc., vol. 15, no. 4, Oct. 1970.
3. Mechtly, E. A.: The International System of Units – Physical Constants and Conversion Factors. NASA SP-7012, 1964.
4. Heyson, Harry H.: Theoretical Study of Conditions Limiting V/STOL Testing in Wind Tunnels With Solid Floor. NASA TN D-5819, 1970.
5. Heyson, Harry H.: Ground Effect for Lifting Rotors in Forward Flight. NASA TN D-234, 1960.
6. Lynn, R. R.; Robinson, F. D.; Batra, N. N.; and Duhon, J. M.: Tail Rotor Design. Part 1 – Aerodynamics. [Preprint No. 300], 25th Annual National Forum Proceedings, Amer. Helicopter Soc., May 1969. (Also J. Amer. Helicopter Soc., vol. 15, no. 4, Oct. 1970, pp. 2-15.)
7. Jenkins, Julian L., Jr.: Trim Requirements and Static-Stability Derivatives From a Wind-Tunnel Investigation of a Lifting Rotor in Transition. NASA TN D-2655, 1965.
8. Heyson, Harry H.: The Flow Throughout a Wind Tunnel Containing a Rotor With a Sharply Deflected Wake. Proceedings Third CAL/AVLabs Symposium, Aerodynamics of Rotary Wing and V/STOL Aircraft, Vol. II, June 1969.

NASA-Langley, 1971 —— 11 L-7432

NATIONAL AERONAUTICS AND SPACE ADMINISTRATION
WASHINGTON, D.C. 20546

OFFICIAL BUSINESS

FIRST CLASS MAIL

POSTAGE AND FEES PAID
NATIONAL AERONAUTICS AN
SPACE ADMINISTRATION

02U 001 26 51 3DS 71070 00903
AIR FORCE WEAPONS LABORATORY /WLOL/
KIRTLAND AFB, NEW MEXICO 87117

ATT E. LOU BOWMAN, CHIEF,TECH. LIBRARY

POSTMASTER: If Undeliverable (Section 158 Postal Manual) Do Not Retur

"The aeronautical and space activities of the United States shall be conducted so as to contribute . . . to the expansion of human knowledge of phenomena in the atmosphere and space. The Administration shall provide for the widest practicable and appropriate dissemination of information concerning its activities and the results thereof."

—NATIONAL AERONAUTICS AND SPACE ACT OF 1958

NASA SCIENTIFIC AND TECHNICAL PUBLICATIONS

TECHNICAL REPORTS: Scientific and technical information considered important, complete, and a lasting contribution to existing knowledge.

TECHNICAL NOTES: Information less broad in scope but nevertheless of importance as a contribution to existing knowledge.

TECHNICAL MEMORANDUMS: Information receiving limited distribution because of preliminary data, security classification, or other reasons.

CONTRACTOR REPORTS: Scientific and technical information generated under a NASA contract or grant and considered an important contribution to existing knowledge.

TECHNICAL TRANSLATIONS: Information published in a foreign language considered to merit NASA distribution in English.

SPECIAL PUBLICATIONS: Information derived from or of value to NASA activities. Publications include conference proceedings, monographs, data compilations, handbooks, sourcebooks, and special bibliographies.

TECHNOLOGY UTILIZATION PUBLICATIONS: Information on technology used by NASA that may be of particular interest in commercial and other non-aerospace applications. Publications include Tech Briefs, Technology Utilization Reports and Technology Surveys.

Details on the availability of these publications may be obtained from:

SCIENTIFIC AND TECHNICAL INFORMATION OFFICE

NATIONAL AERONAUTICS AND SPACE ADMINISTRATION

Washington, D.C. 20546